Joint European Research Infrastructure Network for Coastal Observatories

JERICO WP10.3

Report on Data Analysis (Moored Profile comparisons, 3D T/S structure)

Grant Agreement n° 262584

Project Acronym: JERICO

Project Title: Towards a Joint European Research Infrastructure network for Coastal Observatories

Coordination: P. Farcy, IFREMER,

jerico@ifremer.fr, www.jerico-fp7.eu:

Authors: P Gaughan, M Mowlem, I Puillat, P Farcy, M. Haller, W. Petersen, G. Nolan, K. Sørensen, P. Jaccard, B. Karlson, S. Kaitala, M.C. Hartman, G. Petihakis

Involved Institutions: Marine Institute, Ifremer, NOC, NIVA,HCMR, INSU, SMHI, NERC

Version and Date: Version 1.4 April 2015

TABLE OF CONTENTS

1. Document Description

1.1. REFERENCES

Annex 1 to the Contract: Description of Work (DoW) version of the 22 Feb. 2011

DOCUMENT INFORMATION	
Document Name	WP10 Deliverable 10.3 - Report on Data Analysis
Document ID	WP10 Deliverable 10.3
Revision	4
Revision Date	April 2015
Author	P. Gaughan, G. Nolan , M. Hartman M.Ntoumas, L.Coppola, , M Mowlem, I Puillat, P. Farcy, M. Haller, W. Petersen, G. Nolan, K. Sørensen, P. Jaccard, B. Karlson, S. Kaitala, M.C. Hartman, G. Petihakis
Security	

HISTORY			
Revision	Date	Modification	Author
1.0	16/9/2014	First Draft	P. Gaughan
1.1	1/11/2014	Included inputs from Mark Mowlem	P.Gaughan
1.2	3/3/2015	Included inputs from Rajesh and Laurent	P.Gaughan
1.3	20/4/2015	Included SMHI/NIVA inputs and final draft	P.Gaughan

DIFFUSION LIST				
Consortium beneficiaries	X			
Third parties				
Associated Partners				
Other				

2. Executive Summary

This report focuses on Data analysis and processing techniques undertaken by JERICO partners, it also includes details on the data analysis of a number of inter-comparisons between various sensing technologies including:

- Data analysis Report on Dissolved Oxygen sensors inter-comparison exercises
- A Data analysis and evaluation on Star-Oddi and NKE probes in order to assess their capability to be used for physical oceanography purposes.
- Data analysis, methodological development and 3D T/S (Temperature/Salinity) structure along FerryBox lines carried out under the JERICO project.
- A report on a moored profile analysis trial to assess the data availability using different methods in varying weather and operating conditions and to compare profile measurements from a moored buoy with similar profiles from profiling floats, standard ship based CTD measurements and surface data from FerryBox systems.

These data analysis experiments presented are assessed and presented under the following headings:

- Data collection methodology
- Quality assurance applied
- Analysis
- Scientific results
- Published papers (included as annex)

The real time quality control of operational observation data of a number of Jerico partners has also been addressed with the focus on FerryBox systems. Real time quality controls (RTQC) procedures have been formulated and presented. For all kinds of platform there are general tests applicable. For FerryBoxes some additional tests are also presented here. There is a general agreement in the community for adoption of data quality tests; however, the range of tests is not entirely consistent. Tests are performed either directly on board in real-time or later in the data base on land. For the delayed mode quality control water samples are strongly recommended. Automation of this step remains a difficult task as expert judgement is needed. The topics described are presented as according to the Description of Work (DoW)

- Review of data processing undertaken by JERICO partners
- manual intervention in data processing protocols
- development of (Matlab code) algorithms for data processing

3. Data analysis report on Dissolved Oxygen sensors and inter-comparison exercises

3.1.1. Data collection methodology

Different Dissolved Oxygen (DO) sensors have been inter-compared at the Observatoire Océanologique de Villefranche-sur-mer (OOV, CNRS, France). Two field experiments were realized in the Villefranche Bay (one in October 2013 and one in December 2013), using several types of DO sensors.

- Classic sensor (electrode membrane):
    - 1 SBE 43 (OOV-CNRS, France).
- Optical sensors:
    - 1 optode SBE 63 (M.I.O./CNRS, France),
    - 1 optode Aanderaa 3975 (HCMR, Crete),
    - 1 optode Aanderaa 4330 oxygen optode (OOV-CNRS, France),
    - 1 HOBO U26 ONSET (MI, Ireland)

Each time, a vertical DO profile has been associated with a CTD profile (SBE 19+) with water sampling for Winkler titration (used as O2 concentration reference).

15-Oct-2013

Just before the JERICO WP10 meeting at Villefranche-sur-mer, Laurent Coppola (OOV), Emilie Diamond (OOV), Ingrid Puillat (IFREMER) and Manolis Ntoumas (HCMR) performed a sea experiment for testing accuracy and precision of existing DO sensors but using different technologies and calibration procedures. For this experiment, we used a SBE 43 and a SBE 63 (connected directly on the SBE 19+) and two different Aanderaa optodes (autonomous).

The first cast was realized with the SBE 19+/ SBE 43/ SBE 63 unit (Figure 1) near the EOL buoy in the Villefranche Bay with a 30min stage at 25m. Then seawater was sampled at 25m depth via a Niskin bottle to get three Winkler samples.

Two other casts were performed at 6 m depth with the same unit and using firstly an optode 3975 (Figure 2) and secondly an optode 4330 (Figure 3). These optodes were directly connected to a PC on board. Three other Winkler samples have been taken from a Niskin bottle at 6 m.

The water samples were analysed later with the Winkler method, using a Metrohm 702 SM Titrino potentiometric titration.

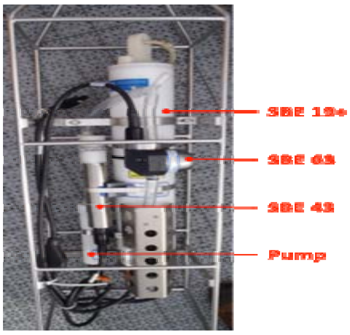

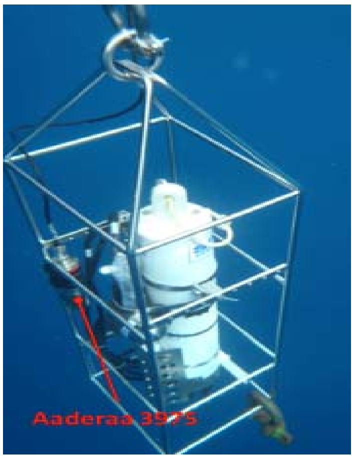

Figure 1: *Autonomous CTD/DO used for JERICO inter-comparison exercise (SBE 19+/ SBE 43/ SBE 63)*

22-Oct-2013

A second experiment has been performed later in October 2013 at the same location (Villefranche bay). On this cast, we deployed a SBE63 sensor on the SBE19+ and we mounted on parallel the HOBO sensor working autonomously. The cast was deployed at 50m depth for 30 min inter-comparison exercise. We collected as well 3 bottles for Winkler measurements.

16-Dec-2013

Another cast was realized near the EOL buoy in the Villefranche Bay, but this time with a 20min stage at 50m and added to the SBE 19+/ SBE 43/ SBE 63 unit, the autonomous HOBO U26 (Figure 4) Then sea water was sampled at 50m via a Niskin bottle to get three Winkler samples analysed two days later.

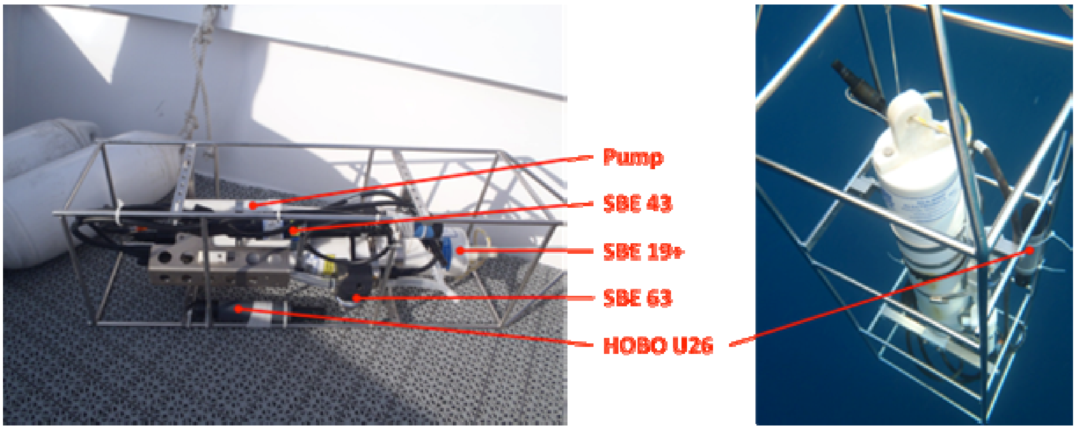

Figure 4 *Autonomous CTD/DO used for JERICO inter-comparison exercise (SBE 19+/ SBE 43/ SBE 63/ HOBO U26)*

3.1.2. Quality assurance applied

All casts were deployed at 30 minute intervals for the intercomparison exercises.

3 samples were collected for redundant purposes for the sea water sample collection

3.1.3. Analysis and Scientific results

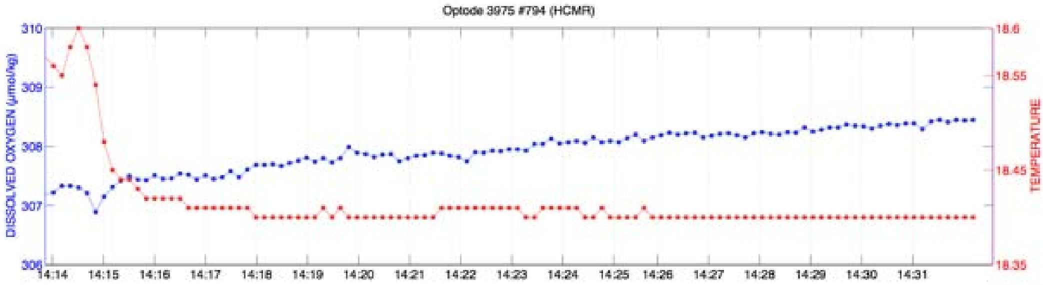

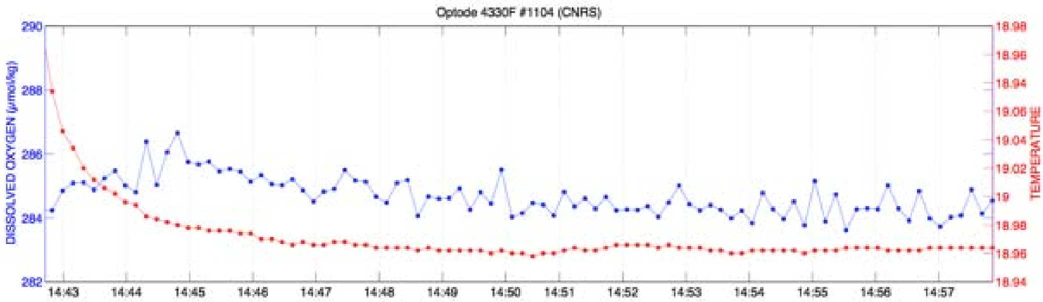

Figure 5 ***Oxygen results for the 2 optodes deployed in surface waters in October 15th. The Winkler measurements at this depth ranged around 245-250 µmol/kg.***

The two optodes (3975 and 4330) showed different results during the deployment. First of all, in between the two optodes, we observed an offset of 20 µmol/kg. The different performance between the two optodes might explain this discordance. For example, the new foil installed on optode 4330 provides a faster time response than the optode 3975 (Figure 5). This could explain the larger variability of O2 concentrations observed on the optode 4330 data. Secondly, the new multi-point calibration procedure performed by the manufacturer improved the quality and the accuracy of the optode 4330 measurements. Compare to the O2 reference value (Winkler titration indicated an oxygen concentration around 245-250 µmol/kg), we observed a large offset ranging from 35 to 55 µmol/kg for optode 4330 and optode 3975, respectively. Even if the results from the optode 4330 is better than those from optode 3975, this offset is too large to be due to natural variability. Such offset for both optodes could be explained by a too old calibration procedures and a long storage of sensors to the dry air condition.

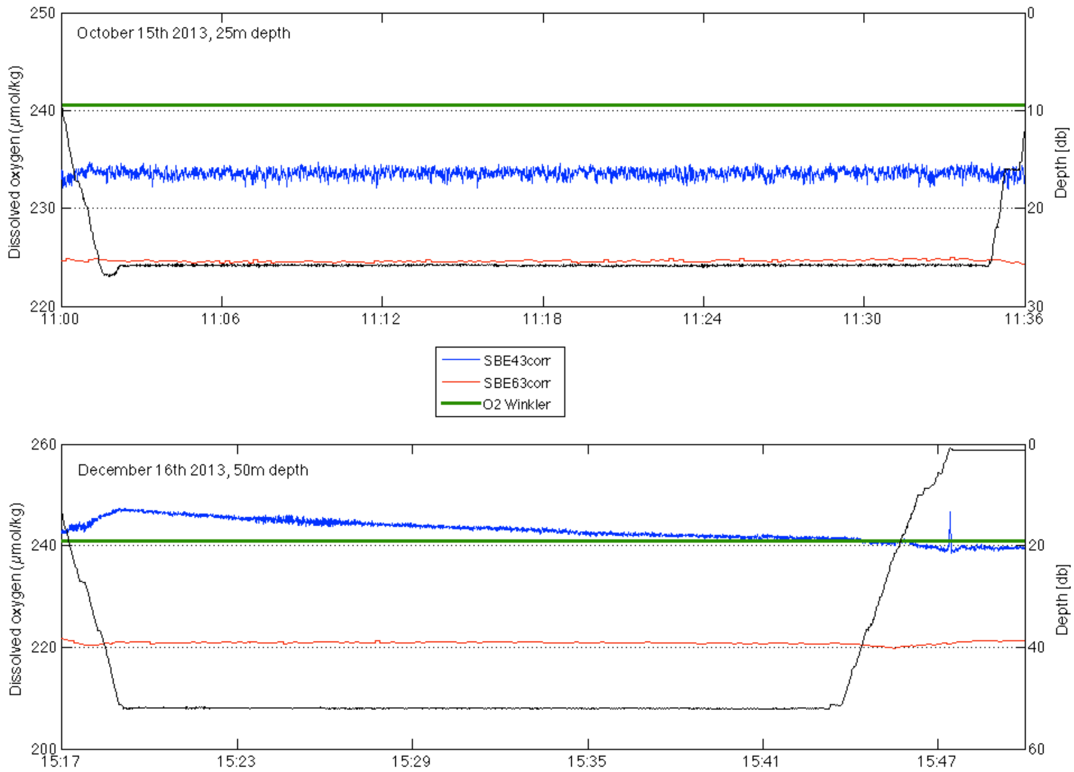

Figure 6: ***Results for SBE43 and SBE63 sensors deployed at 25 and 50m depth in the Villefranche-sur-Mer bay. The green line represents the Winkler reference.***

Results from the two SBE sensors indicate also a disagreement. However, the SBE43 data after correction (adjustment of the SOC slope coefficient) show a better response compared to the SBE63 (adjustment of T, P and S) for the two deployments (Figure 6). The recent yearly calibration of the SBE43 could explain this difference. On the other hand, the SBE63, which corresponds to an optode, is very sensitive to the dry air temperature and the long storage before the deployment. This might explain the observed offset between SBE63 data and the O2 Winkler reference value (20 µmol/kg). However, the capacity of the optode to not drift over the long deployment could give an advantage to this sensor compared to the SBE43 very sensitive to the biofouling and the cleaning procedure.

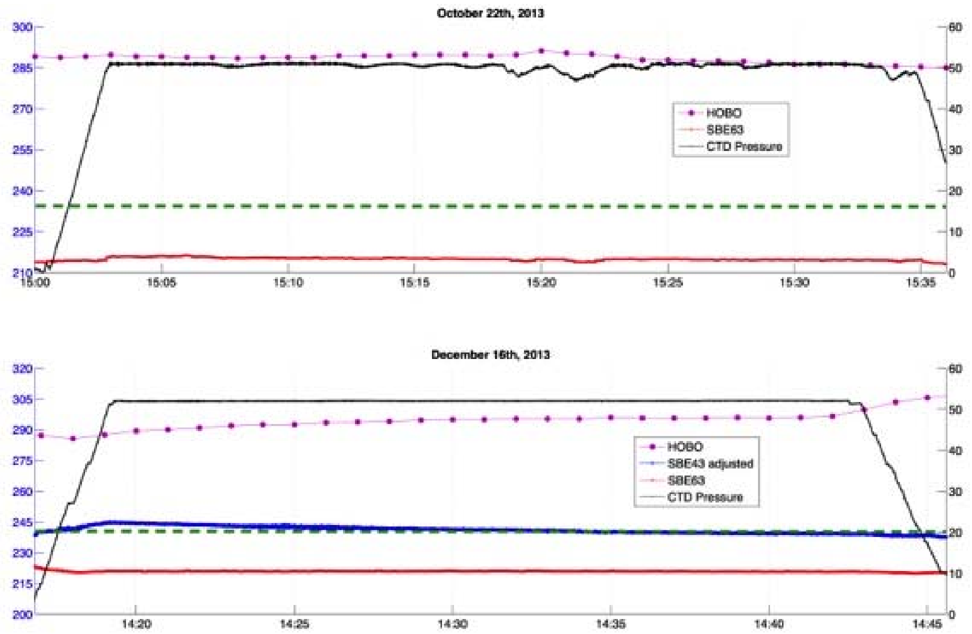

Figure 7 ***Oxygen measurements from HOBO compared to SBE43 and SBE63 sensors deployed in October 22th and December 16th. The dashed green line represents the Winkler reference measurements (234 and 241 µmol/kg, respectively)***

The HOBO sensor from ONSET (optical sensor) was compared to the two SBE sensors and the *in situ* Winkler measurements. It's obvious that the HOBO shows a large offset of 70 µmol/kg compared to the oxygen reference value (Winkler) due to the low accuracy of the sensor (0.2 mg/L = 6 µmol/kg), the low cost factory calibration and probably the too long lasting calibration procedure. However, even the frequency acquisition of the HOBO sensor is less than the SBE sensors (one minute instead one second for the SBE sensors), the stability of the O2 signal seems to be adequate for long-term measurements.

3.1.4. Published Papers

No papers have been published yet based on these inter-comparisons.

4. Data analysis on the Star-Oddi and NKE probes

One of the objectives of JERICO task 10.3 was the evaluation of the data collected by existing commercial sensors to be installed on vessels of opportunity (VOOs), including fishing vessels. This report is specifically aimed at reporting on the evaluation performed on the Star-Oddi and NKE probes in order to assess their capability to be used for physical oceanography purposes.

4.1.1. Data collection methodology

Since 2003, CNR-ISMAR is running a program aimed at using Italian fishing vessels as VOOs for the collection of scientifically useful datasets. In the framework if the EU-FP5 project MFSTEP, 7 commercial vessels fishing for small pelagic species in the northern and central Adriatic Sea were equipped with an integrated system for the collection of data regarding catches, position of the fishing operation, depth and water temperature during the haul (Falco et al. 2007); this system was named "Fishery Observing System" (FOS) and until 2013 produced a great amount of data that, could be helpful both for oceanographic and fishery biology purposes (Falco et al 2011; Martinelli et al. 2012; Sparnocchia et al 2013).

In 2013 CNR upgraded the FOS to FOOS, the Fishery & Oceanography Observing System (Martinelli et al. 2013). New sensors for the collection of oceanographic and meteorological data allow nowadays the FOOS to collect more parameters, with higher accuracy, and to send them directly to a data center in near real time. The FOOS represents thus a multifunction system able to collect data from the fishing operation and to send them to an inland data center, but also to send back to the fishermen useful information, as for instance weather and sea forecasts, etc. through an electronic logbook with an ad hoc software embedded (Patti et al. 2013). The FOOS implementation allowed a spatial extension of the monitored area and the installation on various kind of fishing vessels such as coupled pelagic trawlers, bottom trawlers, purse seiners etc. This point is of particular interest because of the multiplicity of fishing gears used in the Mediterranean and the variety of target species and exploited areas.

This report is specifically aimed at reporting on the data collected by the Star-Oddi and NKE probes in order to assess their capability to be used for physical oceanography purposes. The sensors mounted on fishing gears can retrieve, almost daily, a huge amount of physical data, such as temperature, depth and salinity, spanning a very large spatial region both horizontally and vertically.
The possibility of establishing the accuracy of these data would be of extreme importance for physical oceanography studies since it would be almost impossible to obtain the same amount of data with normal cruises onboard a R/V.

In order to accomplish this task, tests were performed in the Adriatic Sea during several surveys taking place on board of R/V Dallaporta within the JERICO project duration; furthermore also data previously collected were used in order to achieve the results reported in this document, which are related to the performances of several StarOddi and NKE sensors compared to those of a calibrated CTD instrument.

4.1.2. Analysis

4.1.2.1. Profile examples

An example of depth profile for a cast of two FOS-FOOS sensors (a Star-Oddi and an NKE) and the CTD instrument is shown in Fig.8. In this graph, we have indicated the data range in which the data depth mode for each sensor was calculated. In correspondence of this data range, the temperature and salinity modes were also calculated, when appropriate.

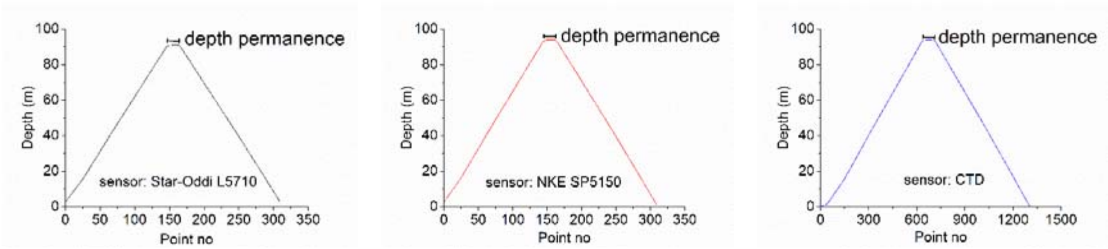

Figure 8 Examples of depth profile for Star-Oddi (left), NKE (center), CTD (right) probes. For each profile, the depth permanence is indicated. The cast was performed on March 2nd 2012 at 9:23am. Note the different data acquisition rate (number of poin

In Fig.8, the temperature-depth profiles relative to the casts of Fig.2 are reported on the same graph to show the difference between the readings of the different sensors. For a better readability, only the descendent part of the cast is considered. The profile of another NKE sensor with salinity measurement capability (STPS31004) was added to this graph.

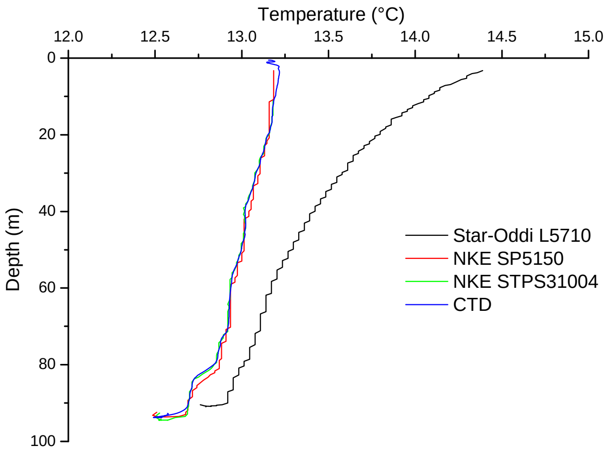

Figure 9 Temperature-depth profile of four different sensors (same cast as Fig. 1). Only the descent part of the cast is shown.

The different temperature time response between the Star-Oddi sensor and the other sensors prevented the use of the whole data profile to evaluate the offset reading. The NKE sensor readings are much more consistent with the CTD reading. However, due to the temperature and depth accuracy and different time response of the temperature sensors, in order to evaluate a precise offset of sensor it was established to calculate the sensor offsets only during the permanencies at constant depth where no transient effects are present.

An example of salinity profile for three NKE sensors and CTD is shown in Fig.9. In this case all the NKE profiles are altogether shifted towards lower values and are much noisier than that of the CTD instrument. While the offset is clearly due to the sensor accuracy, the more spiky behavior is due to the different operating mode of the sensor and the CTD instrument (refer to the Experimental section). A reduction of the spiky NKE reading can be easily achieved by post-processing the raw NKE salinity data with a low-pass filter as it is the case of the CTD data.

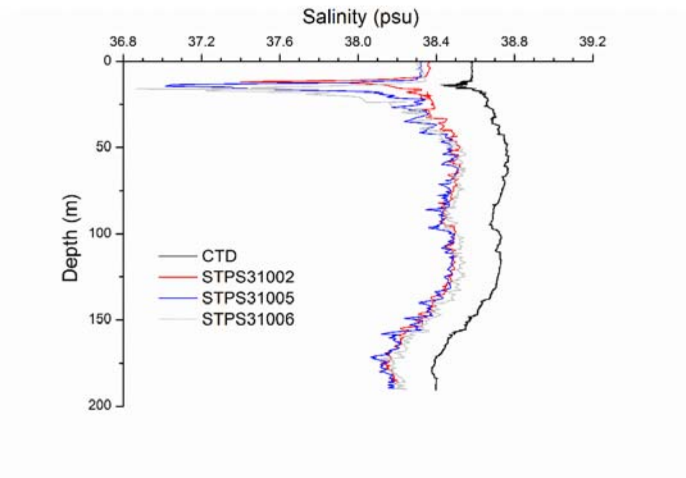

Figure 10. Example of salinity-depth profile for three NKE sensors and CTD instrument (cast date: 22nd July 2011, cast time: 21:56). Only the descent part of the cast is shown. Note the general offset between the NKE sensors and CTD and the more spiky reading of all the NKE sensors

A more striking example of the effects of sensor operating condition on the salinity reading is shown in Fig.10 In this case, the NKE sensors and the CTD instrument were all attached to a sledge which was deployed at the sea bottom (196 m). Once reached the bottom, the sledge was left in place for about 15 min (sledge at rest) and then dragged. When the sledge was at rest the NKE salinity reading was very noisy but when the sledge was dragged, with a regular water flow inside the sensor, the NKE salinity reading stabilized. The different offset of each sensor was instead due to the different sensor accuracy.

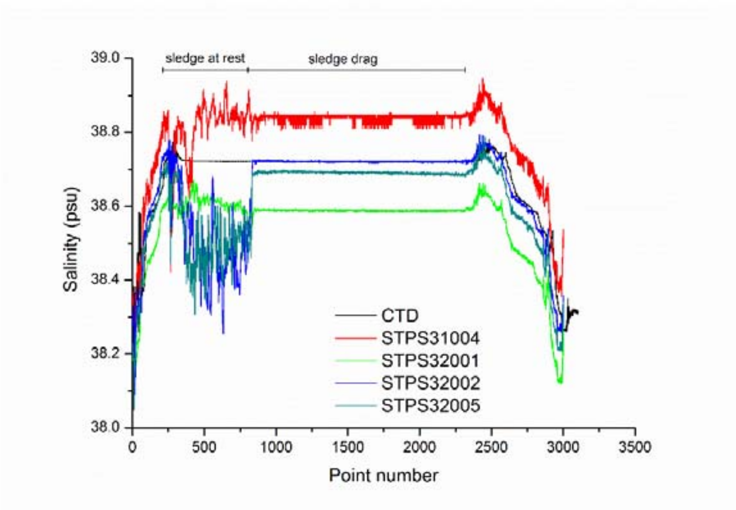

Figure 11 Example of salinity profiles for four NKE sensors and CTD instrument (cast date: 9th May 2014, cast time: 14:24). Note the noisy behavior of the NKE readings when the sledge was at rest and its stabilization when the sledge was dragged.

4.1.2.2. Depth offset of the Star-Oddi sensors

The box plot of Fig.12 shows the depth offset for the Star-Oddi sensors calculated on the whole dataset. We choose the median as statistic for the central tendency of the data as it is less sensitive to outliers. As can be seen, the behavior of the Star-Oddi sensors regarding the depth reading was not consistent from sensor to sensor. The offset median was in fact either positive or negative. Also the offset spread (range between the minimum offset value and maximum offset value) was quite different from sensor to sensor. The offset median of several sensors was outside the accuracy range indicated by the manufacturer with two sensors, L5705 and L3810, showing a very large offset (>7 m).

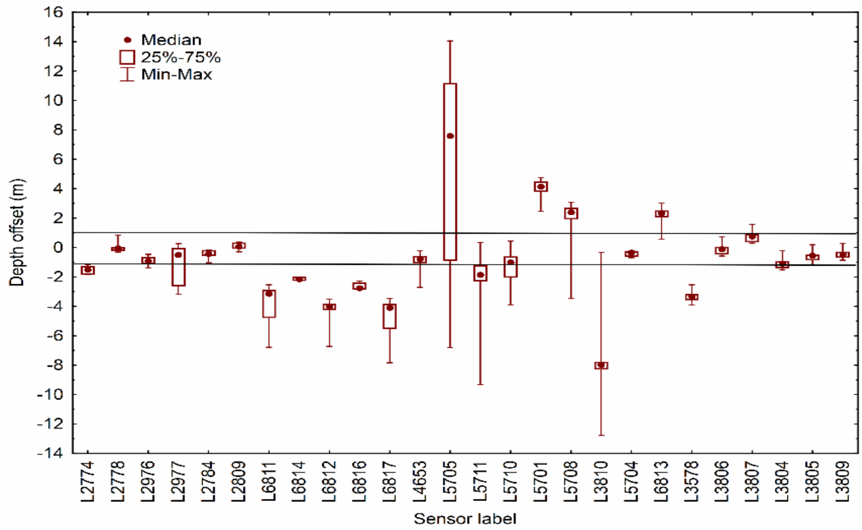

Figure 12 Box plot of the depth offset of the Star-Oddi sensors. The nominal sensor accuracy range is indicated by horizontal lines.

Depth offset could depend on several factors: operating conditions and sensor accuracy. To investigate the behavior of the offset as a function of the cast parameters, the depth offsets of each sensor were analyzed as a function of the cast parameters: depth at depth permanence, dwell time at the depth permanence and temperature at the depth permanence. CTD values of depth and temperature were taken as the true values of these parameters.

If the depth sensor reading of the Star-Oddi probe were influenced by the external pressure, a relationship between the depth offset and the depth at the depth permanence would be statistically significant. The correlation coefficient between the absolute values of the depth offset of the Star-Oddi sensors and the depth at depth permanence is 0.32, which indicates a weak association between the two variables. We have considered the absolute value of the offset to avoid the mutual cancellation between sensors with an opposite sign of the offset. However, the correlation coefficient is appropriate for a linear relationship. A nonlinear relationship would not emerge by considering the correlation coefficient. In Fig. 13, the depth offset of each of the Star-Oddi sensors is plotted as a function of depth at the depth permanence to highlight the performance of any single Star-Oddi sensor. As can be seen, there is no evidence of strongly nonlinear trend of the depth offset with the depth for any of the Star-Oddi sensors. From the graph of Fig.7, it can be said that there was not a unique reading pattern for the Star-Oddi sensors. For small depths, say <100 m, in many cases the Star-Oddi sensor offset tends to decrease when the depth increased. However, also the opposite behaviour was observed, see for example sensor L6816, L5701, L5704. When sensor L5705, L5711 and L3810 were deployed at the same depth but at different casts, i.e. at different times, their offset was not repeatable. When a specific sensor was employed for cast which spanned a large vertical range, the offset was not very consistent, see for example sensor L5705, L5708, L5711 or L3810.

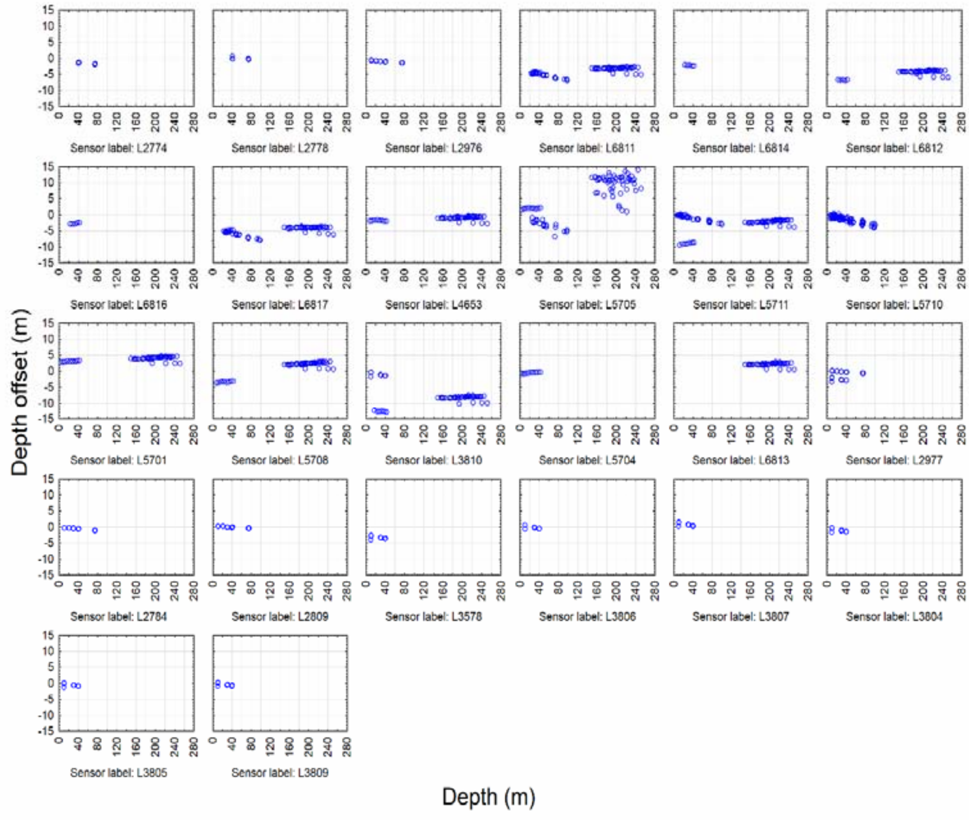

Figure 13 . Depth offset of the Star-Oddi sensors as a function of depth at the depth permanence.

The correlation coefficient of the absolute values of the depth offset with the dwell time is 0.31 which indicates a very weak association between these two variables. The depth offset as a function of the dwell time at the depth permanence is shown in Fig.8 for each Star-Oddi sensor. As it can be seen, in most of the cases the depth offset was nearly independent on the dwell time. A pathological behavior was however observed for sensor L5705, L5711, L5708 and L3810, which were also the sensors with the less consistent behavior of the offset with the depth, see Fig.7.

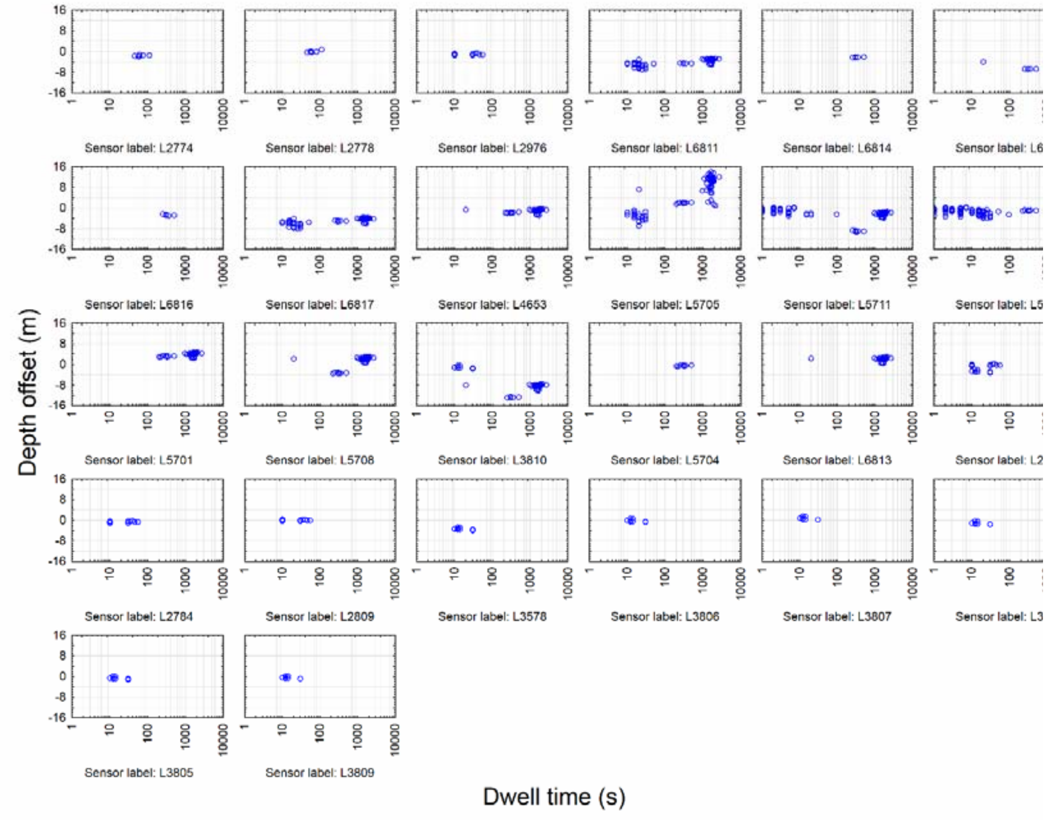

Figure 14 Depth offset of the Star-Oddi sensors as a function of dwell time at the depth permanence.

The correlation coefficient of the absolute values of the depth offset with the temperature at the depth permanence is -0.04 which indicates almost no association between these two variables. The depth offset as a function of temperature at the depth permanence is shown in Fig.14 for each Star-Oddi sensor. As it can be seen, in most of the cases the depth offset was nearly independent on the temperature. Sensors L5705, L5711, L5708, and L3810 have the less consistent behavior.

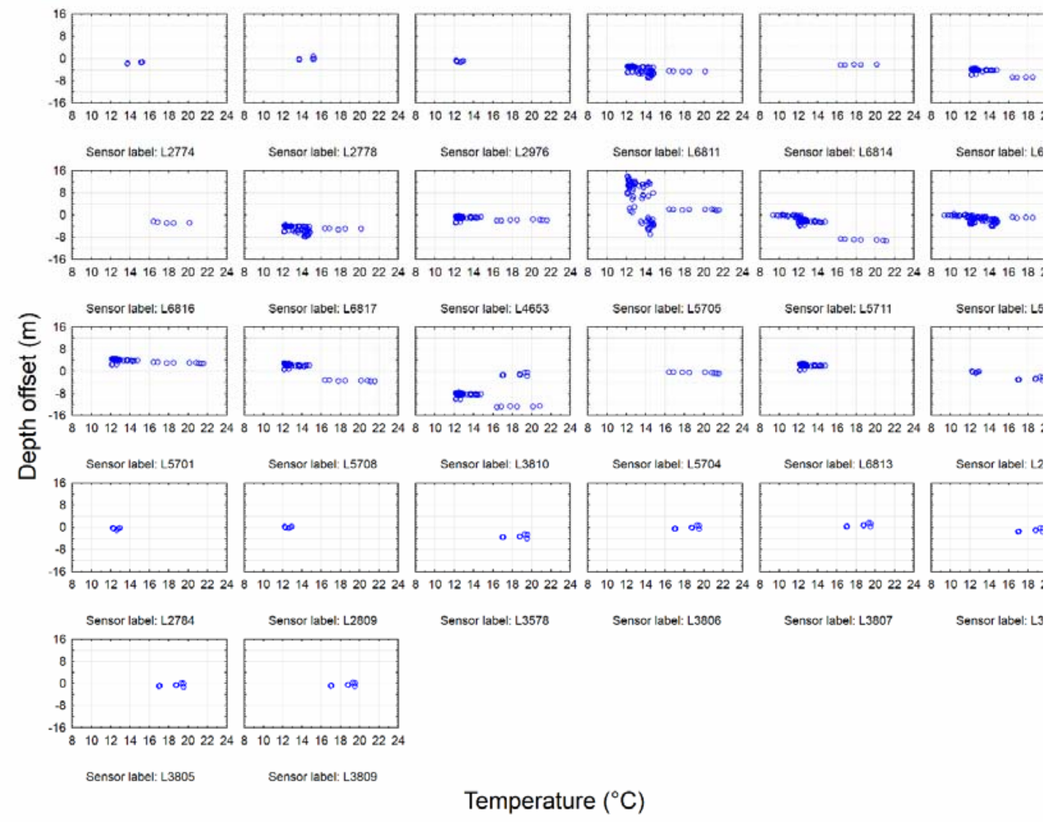

Figure 15. Depth offset of the Star-Oddi sensors as a function of temperature at the depth permanence.

4.1.2.3. Temperature offset of the Star-Oddi sensors

The box plot of Fig.16 shows the temperature offset for the Star-Oddi sensors calculated on the whole dataset. Unfortunately, the sensor L2774, used for only one cast, failed to record the temperature data and its data does not appear in this box plot as well as in the following graphs of this section.

As can be seen, the behavior of the Star-Oddi sensors regarding the temperature reading was much more consistent than in the case of depth. When outside the accuracy range, the offset was always negative. The offset spread (range between the minimum offset value and maximum offset value) was more constant from sensor to sensor with respect to the depth. Only in two cases, sensor L2778 and L2784, the offset was always larger than 1°C. In all the other cases, the median value of the offset was inside the accuracy range or just slightly lower.

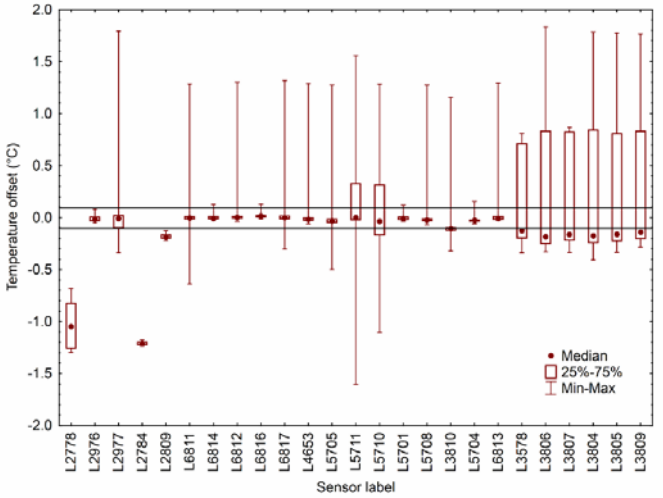

Figure 16. Box plot of the temperature offset of the Star-Oddi sensors. The nominal sensor accuracy range is indicated by horizontal lines.

The correlation coefficient between the absolute values of the temperature offset of the Star-Oddi sensor and the depth at the depth permanence is -0.4 which indicates a moderate association between the two variables. Figure 17 shows the temperature offset for each of the Star-Oddi sensors as a function of depth at the depth permanence. Many sensors showed a nearly constant offset as a function of depth with some occasional distant values. Sensor L5711, L5710, L2977, L3806, L3807, L3804, L3805 and L3809 have a quite large spread of the offset values.

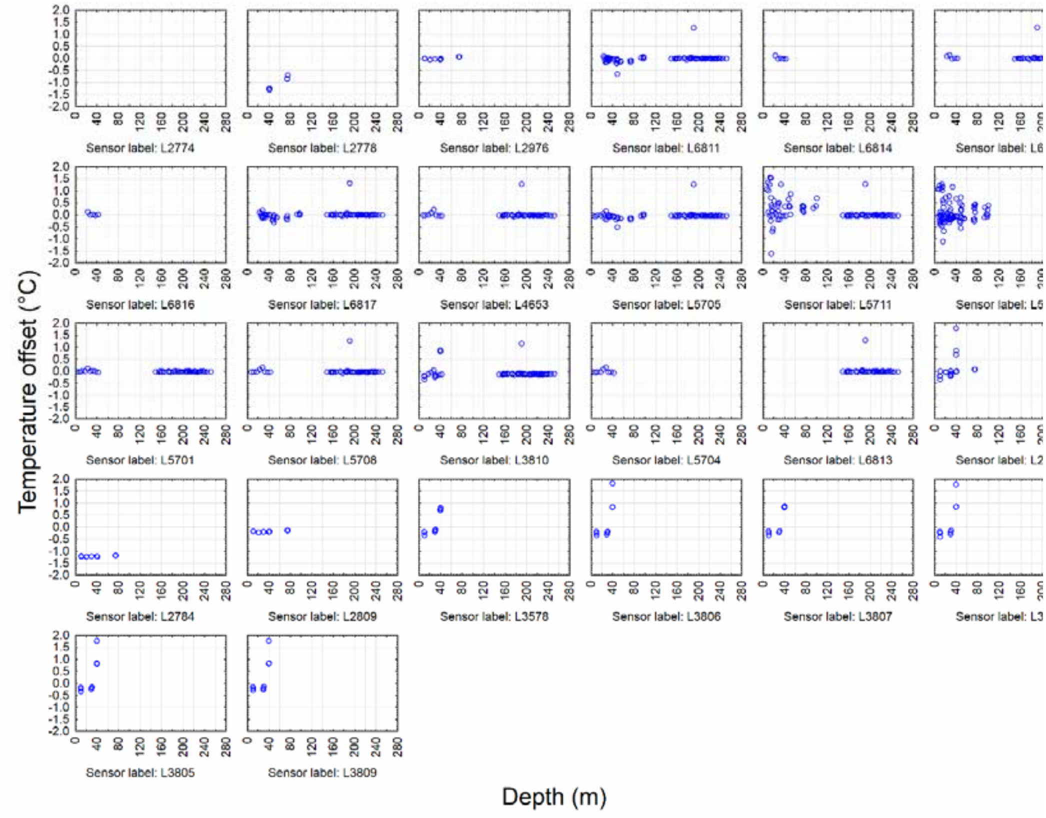

Figure 17. Temperature offset of the Star-Oddi sensors as a function of depth at the depth permanence.

The correlation coefficient between the absolute values of the temperature offset of the Star-Oddi sensor and the dwell time is -0.48 which indicates a moderate association between the two variables. Quite instructive is Figure 13 where the temperature offset is shown as a function of the dwell time for each of the Star-Oddi sensors. As can be see, when the dwell time was higher than, say, 50 s, the temperature offset tend to zero for all the sensors which were tested under these conditions.

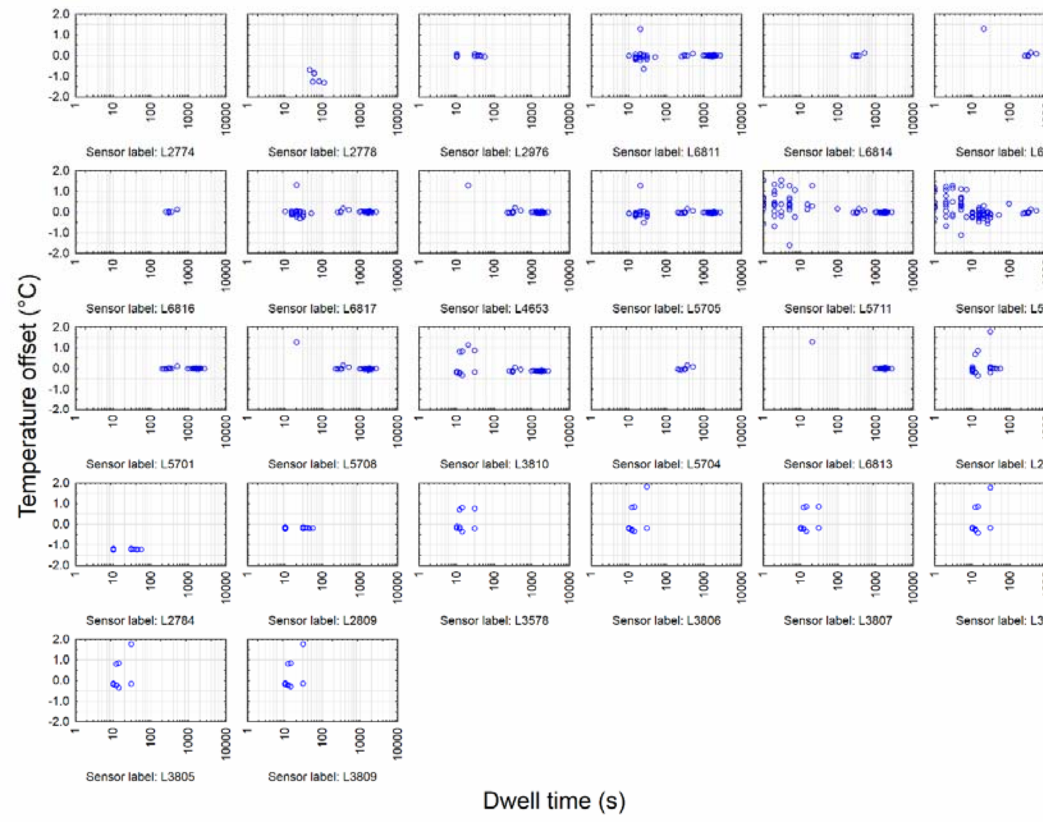

Figure 18. Temperature offset of the Star-Oddi sensors as a function of dwell time at the depth permanence.

According to the manufacturer's information, the temperature offset should have leveled off after about 20 s. From our findings, a longer time (>50 s) is needed for the stabilization of the temperature reading.

If only offset values with dwell time longer than 50 s are considered, the box plot of Fig.19 is obtained. In this case, the offset median is inside the accuracy bonds for all but three Star-Oddi sensors: L2778, L2784, L2809. The greatest portion of the offset values is inside the accuracy range. Besides an influence on the median values, also the offset spread was also greatly reduced by considering longer dwell times.

Note in passing that the moderate association calculated between the temperature offset and the depth at depth permanence is definitely due to the very strong association between the dwell time and depth (correlation coefficient: 0.91).

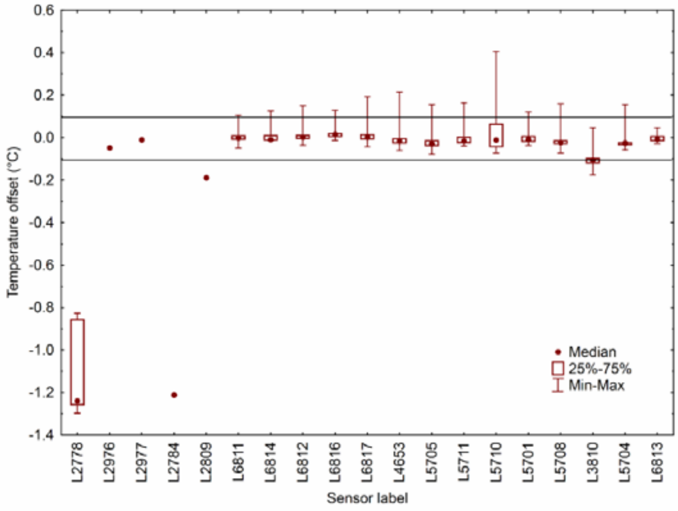

Figure 19. Box plot of the offset of the Star-Oddi sensors with a dwell time at the depth permanence longer than 50 s. The nominal sensor accuracy range is indicated by horizontal lines. Compare with Fig.11.

The correlation coefficient between the absolute values of the temperature offset of the Star-Oddi sensor and the temperature at the depth permanence is 0.01 which indicates absence of the relationship between the two variables. Figure 20 shows the temperature offset for each of the Star-Oddi sensors as a function of temperature at the depth permanence.

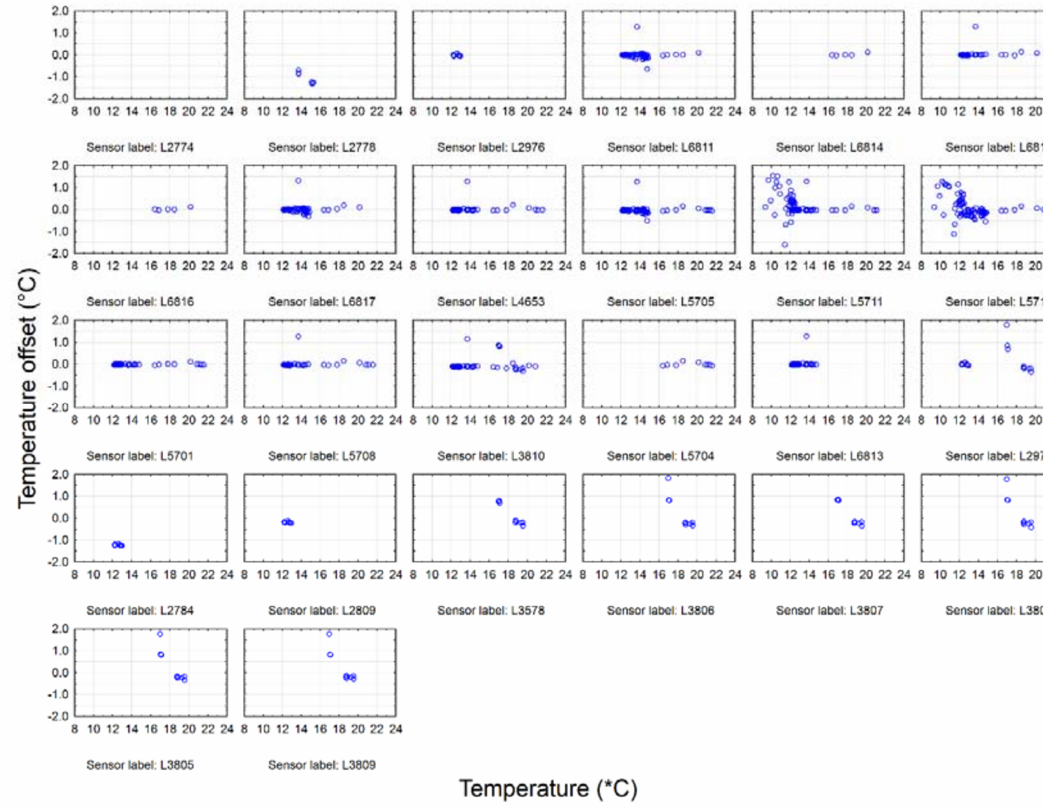

Figure 20. Temperature offset of the Star-Oddi sensors as a function of temperature at the depth permanence

In most cases, the temperature offset of the Star-Oddi sensors is independent on the temperature at the depth permanence. Some sensors (L6811, L5711, L5710, L2977, L3578, L3806, L3807, L3804, L3805, L3809) seem to have a more accurate reading when temperature was higher than 18°C. This is however due to the short permanence time for those casts, see Fig.20.

4.1.2.4. Depth offset of the NKE sensors

The box plot of Fig. 21 shows the depth offset for the NKE sensors calculated on the whole dataset.

As can be seen, the behavior of the NKE sensors regarding the depth reading was more consistent than the Star-Oddi sensors. Only in two cases (STPS31006 and STPST31002) the offset median was well outside the nominal accuracy range. The offset median of Sensor STPS31006 is about -6 m but some values fall inside the accuracy range, while sensor STPST31002 has all the offset values outside the accuracy range but the offset median of this sensor was about -2 m. The offset median of sensor STPS31004 was just above of the accuracy limits. In all the other cases, the offset median was inside the accuracy range with a narrow spread of the values (range between minimum and maximum value).

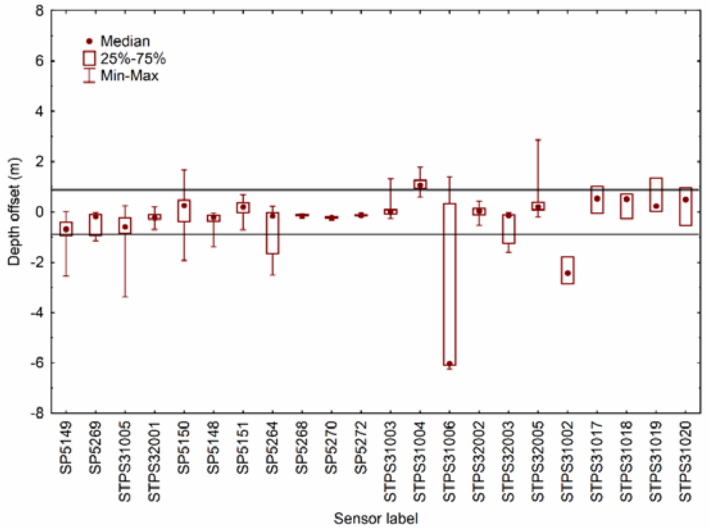

Figure 21. Box plot of the depth offset of the NKE sensors. The nominal sensor accuracy range is indicated by horizontal lines.

The correlation coefficient between the absolute values of the depth offset of the NKE sensor and the depth at the depth permanence is 0.09 which indicates no association or just a very weak one between these two variables. Figure 22 shows the individual offsets of each NKE sensor plotted as a function of depth at the depth permanence. As a general indication, it can be said that the NKE sensor offset was apparently less influenced by the depth with respect to the Star-Oddi sensors. However, also for the NKE sensors, some inconsistent behavior was observed (quite different offset at the same depth), see, for example, sensor SP5149, SP5264, STPS31005, STPS31006, STPS32005.

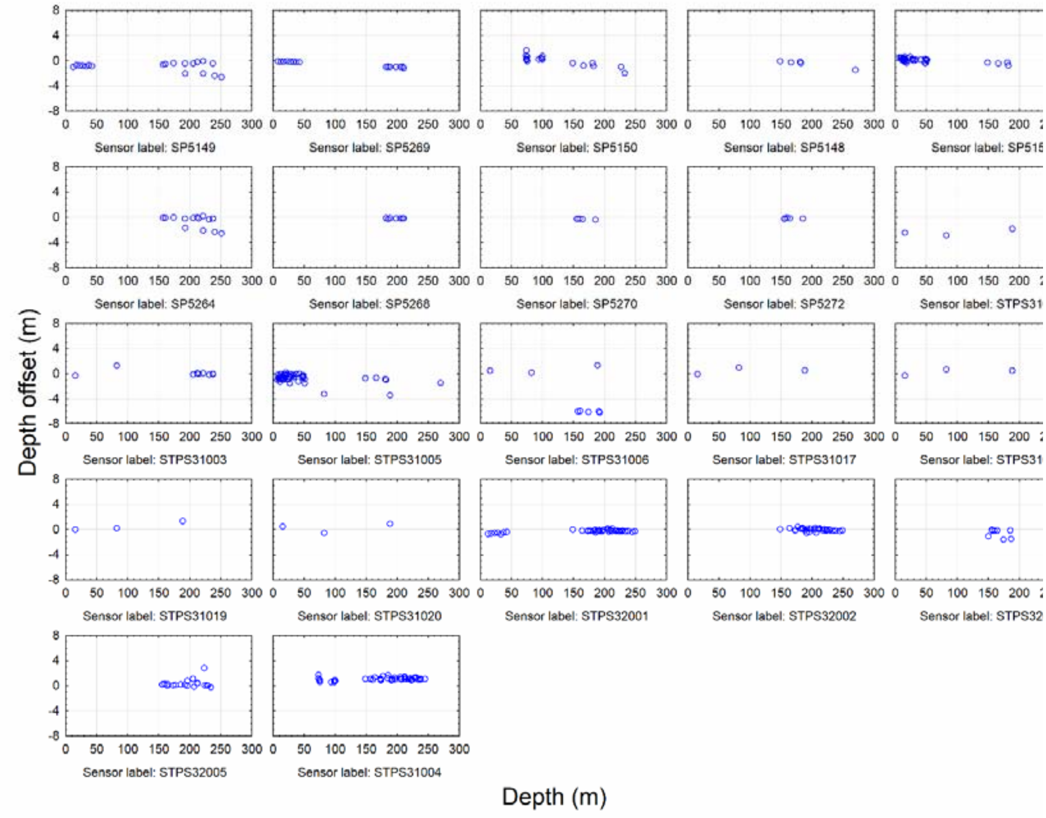

Figure 22. Depth offset of the NKE sensors as a function of depth at the depth permanence.

The correlation coefficient between the absolute values of the depth offset and the dwell time is -0.02 which indicates no association or a very weak one. In Fig. 23, the depth offset of each of the NKE sensors is plotted against the dwell time. The offset values are less spread than in the case of the Star-Oddi sensors and there seems to be no influence of the dwell time on the depth offset.

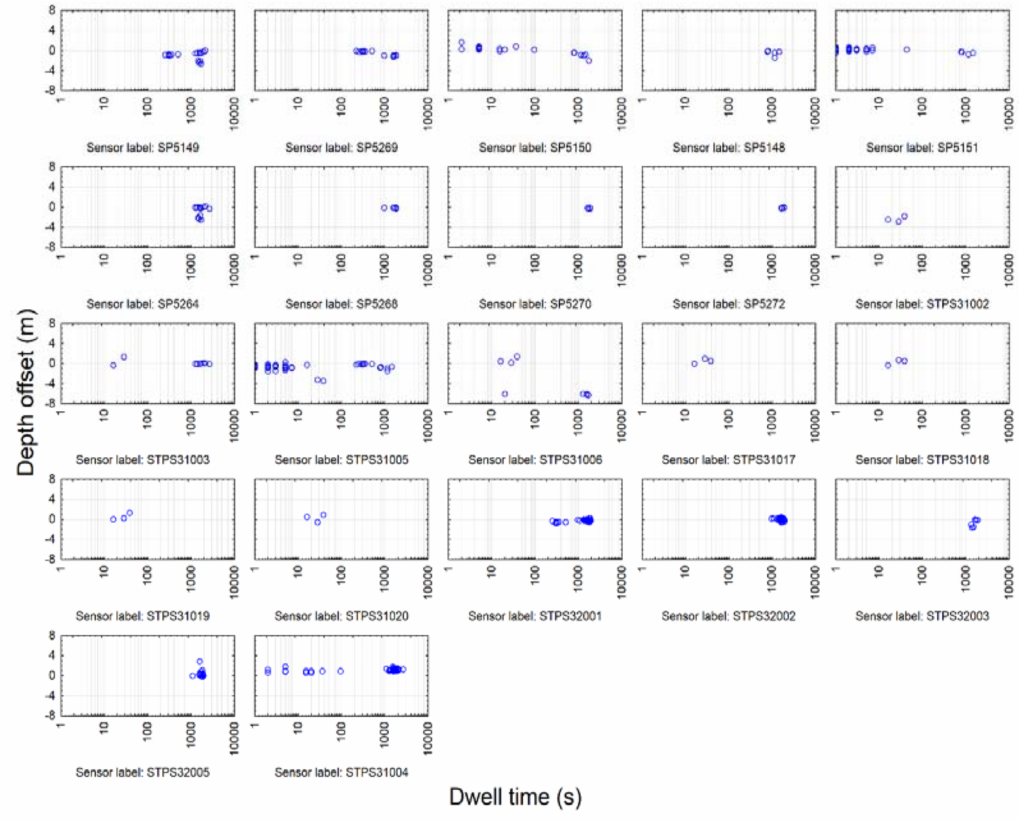

Figure 23. Depth offset of the NKE sensors as a function of dwell time at the depth permanence.

The correlation coefficient between the absolute value of the depth offset and the temperature at the depth permanence of the NKE sensors is -0.06 which indicates no association or a very weak one. In Fig. 19, the depth offset of each of the NKE sensors is plotted against the temperature at the depth permanence.

As can be seen, the depth offset of the NKE sensors was almost independent on the temperature at the depth permanence in all cases. Only sensor STPS31006 shows an unpredictable pattern.

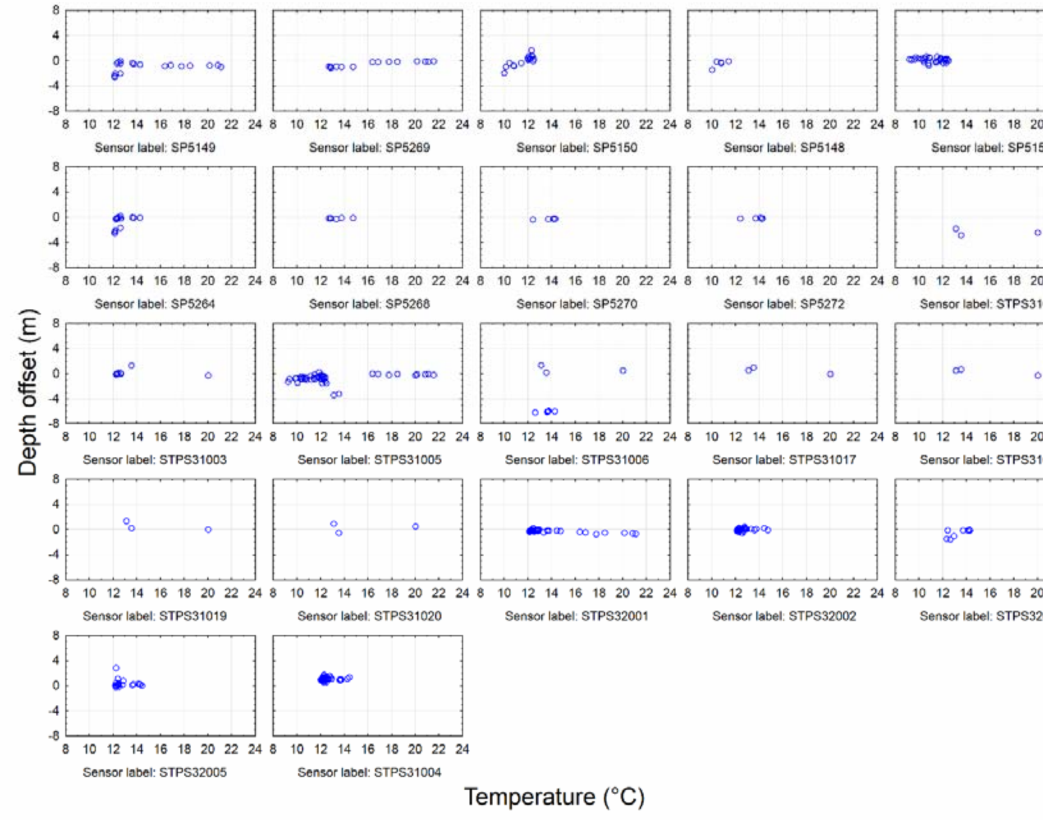

Figure 24. Depth offset of the NKE sensors as a function of temperature.

4.1.3. Temperature offset of the NKE sensors

In Fig.25, the box plot of temperature offset of the NKE sensors is reported.

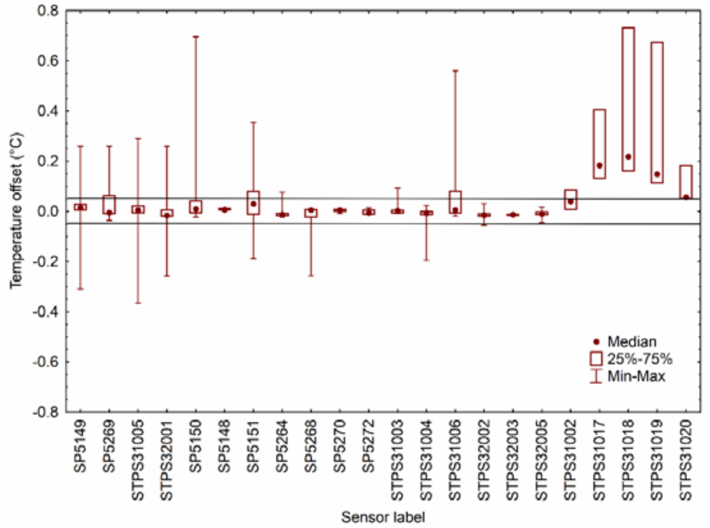

Figure 25. Box plot of the temperature offset of the NKE sensors. The nominal sensor accuracy range is indicated by horizontal lines.

As can be seen, the behavior of the NKE sensors regarding the temperature offset median was quite consistent from sensor to sensor. Only four sensors (STPS31017, STPS31018, STPS31019, STPS31020) have the offset median slightly outside the accuracy range. The spread of the offset values greatly varied from sensor to sensor. However, for the majority of the NKE sensors, most of the offset values fall inside the nominal accuracy range.

The correlation coefficient between the absolute values of the temperature offset of the NKE sensors and the depth at depth permanence is -0.38 which indicates a weak association between the two variables. In Fig.26, the temperature offset is plotted versus the depth at the depth permanence for each of the NKE sensors. Apparently, there is no a visible effect of the depth on the temperature offset of the NKE sensors. Only a larger data spread is usually observed for lower depths.

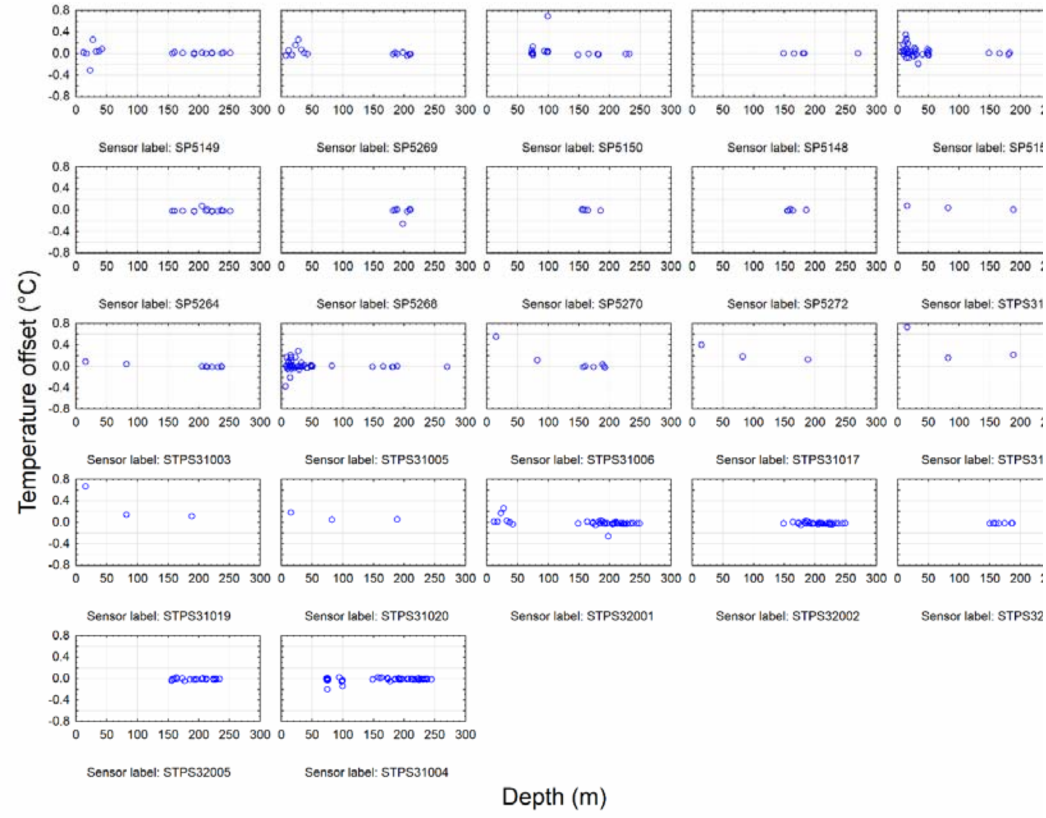

Figure 26. Temperature offset of the NKE sensors as a function of depth at the depth permanence.

The correlation coefficient between the absolute values of the temperature offset and the dwell time is -0.37 which indicates a weak association between the variables. In Fig.26, the temperature offset of each of the NKE sensors is plotted versus dwell time. Even if less evident than in the case of the Star-Oddi sensors, also for the NKE sensors it can be observed that the offset value tends to zero with the increase of the dwell time.

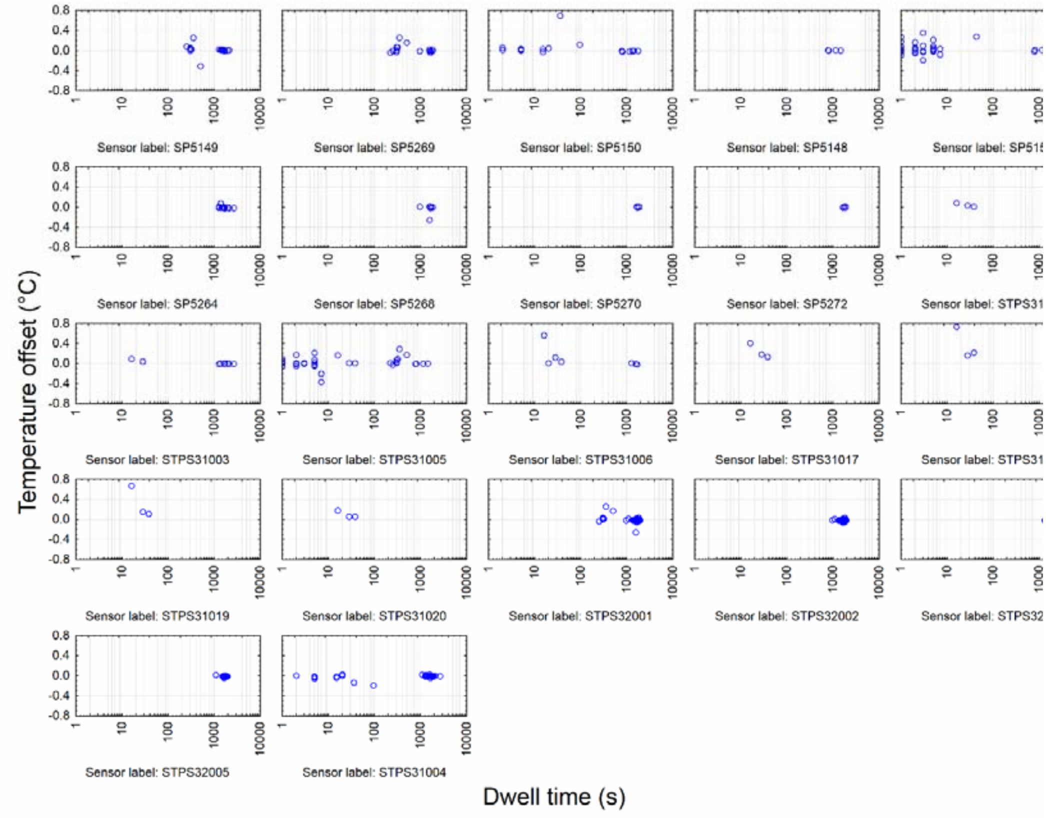

Figure 27. Temperature offset of the NKE sensors as a function of dwell time.

For comparison purposes, in Fig.28 the box plot of the temperature offsets for the NKE sensors is shown for dwell time larger than 50 s. With this selection, all the offset medians and most of the offset values are inside the accuracy range. Note how the offset spread was also greatly reduced.

The weak association between the absolute temperature offset and depth is again due to the strong relationship between depth and dwell time (correlation coefficient: 0.86).

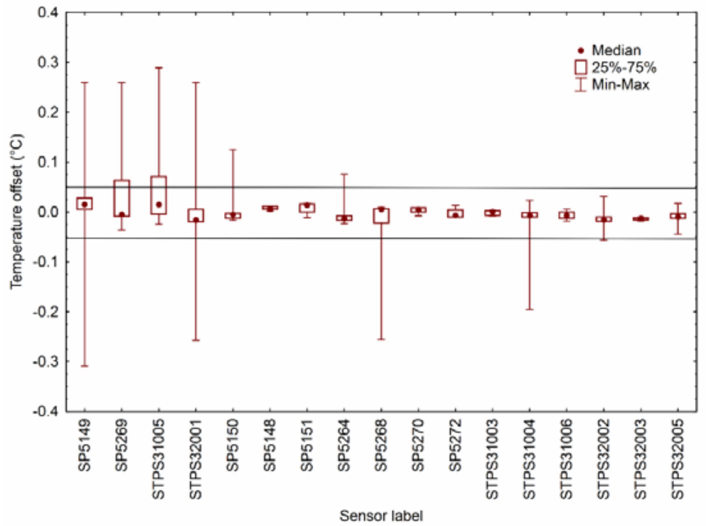

figure 28. Box plot of the temperature offset of the NKE sensors with a dwell time at the depth permanence longer than 50 s. The nominal sensor accuracy range is indicated by horizontal lines. Compare with Fig. 20

The correlation coefficient between the absolute value of the temperature offset and the temperature at the depth permanence is -0.30 which indicates a weak association between the variables. In Fig.28, the temperature offset of each of the NKE sensors is plotted versus temperature at the depth permanence.

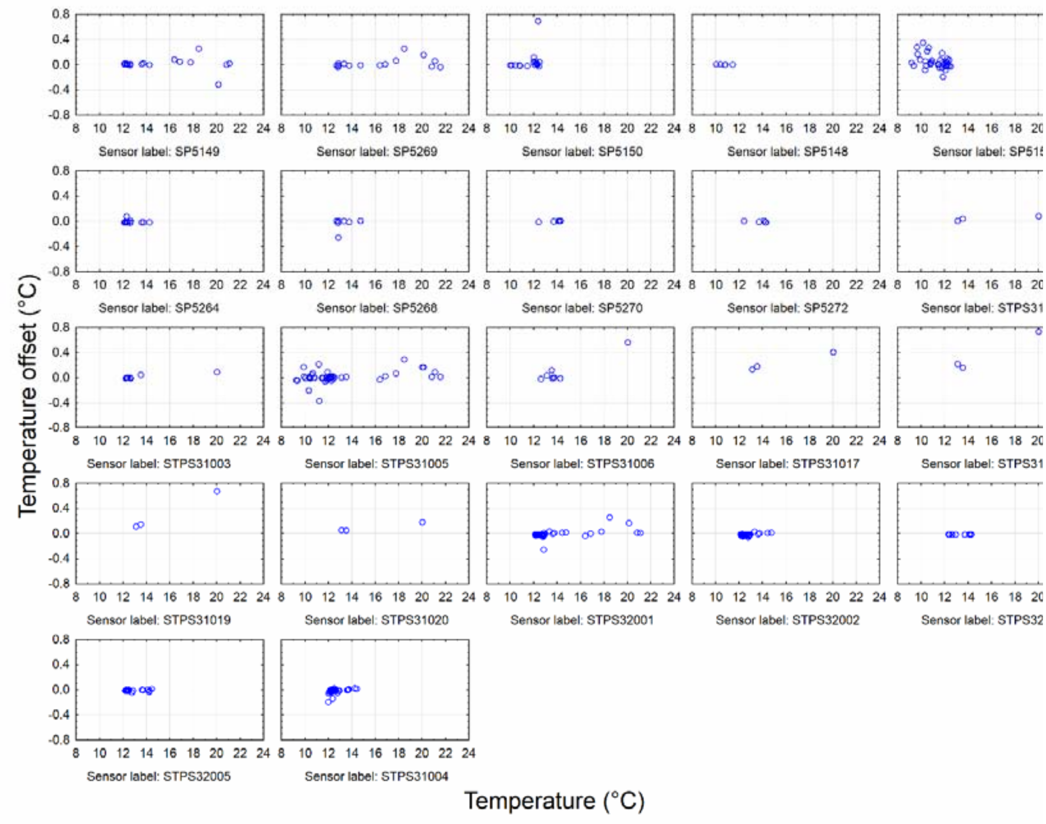

Figure 29. Temperature offset of the NKE sensors as a function of temperature at depth permanence.

Sensor SP5150, STPS31005, STPS31006, STPS31017, STPS31018, STPS31019 have some offset value which would indicate an increase of the offset with the increase of temperature. Also in this case, these values are due to the very short dwell time at the depth permanence, see Fig.29.

4.1.3.1. Salinity offset of the NKE sensors

In Fig.30, the salinity offset for the NKE sensors is shown in the usual box plot style. Five out of eight sensors have the offset median outside the accuracy range declared. The salinity reading was generally lower than the CTD reading (negative offset) with offset spread different from sensor to sensor. In particular, sensor STPS31005 is penalized by a very low value of salinity offset (about -5 psu, not shown).

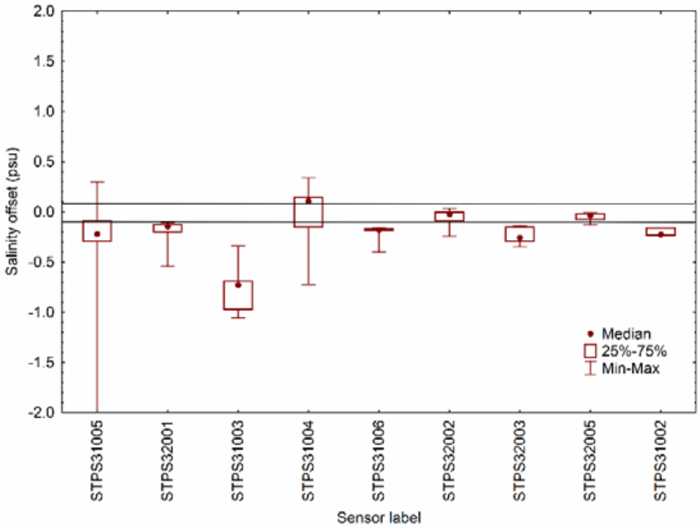

Figure 30. Box plot of the salinity offset of the NKE sensors. The nominal sensor accuracy range is indicated by horizontal lines.

The correlation coefficient between the absolute value of the salinity offset and the depth at depth permanence of the NKE sensors is -0.15 which indicates a weak association between the variables. In Fig.26, the salinity offset is plotted versus depth for each of the NKE sensors. Apparently, there is no influence of the depth on the salinity offset. Also the data spread seems to depth-independent.

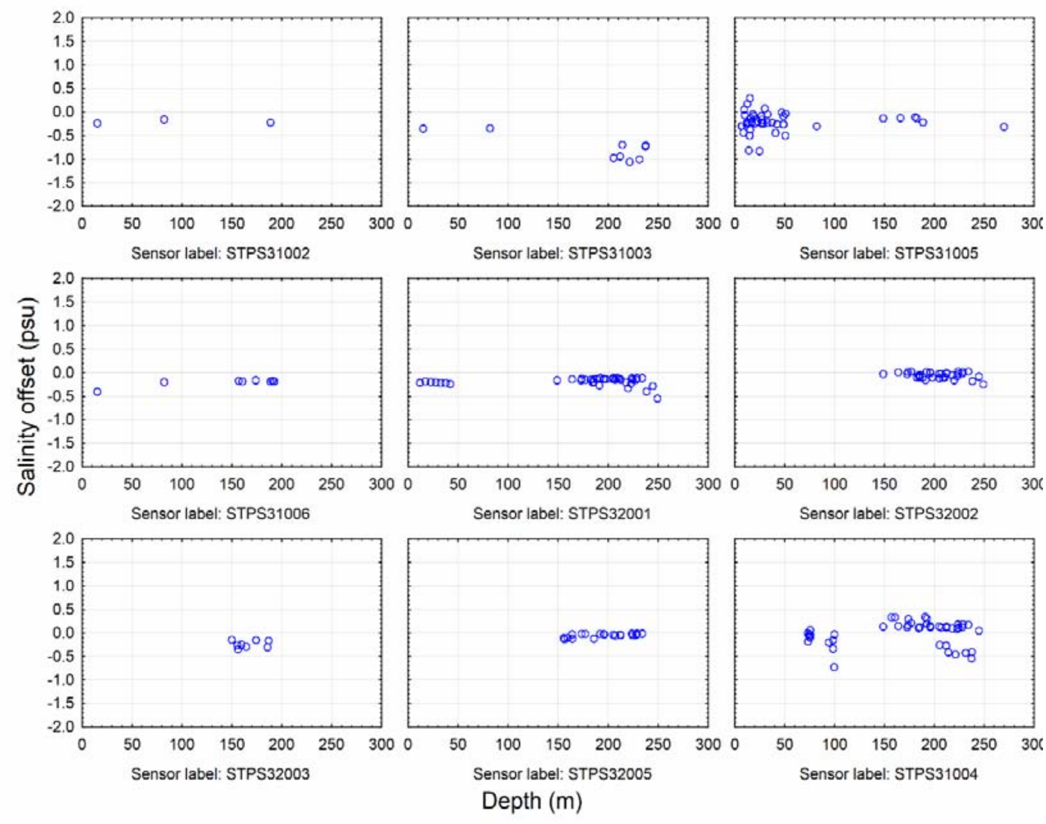

Figure 31. Salinity offset of the NKE sensors as a function of depth at the depth permanence.

The correlation coefficient between the absolute value of the salinity offset and the dwell time of the NKE sensors is -0.13 which indicates a weak association between the variables. In Fig.31, the salinity offset of each of the NKE sensors is plotted versus dwell time. Also in this case, there seems to be no relationship between the salinity offset and the dwell time.

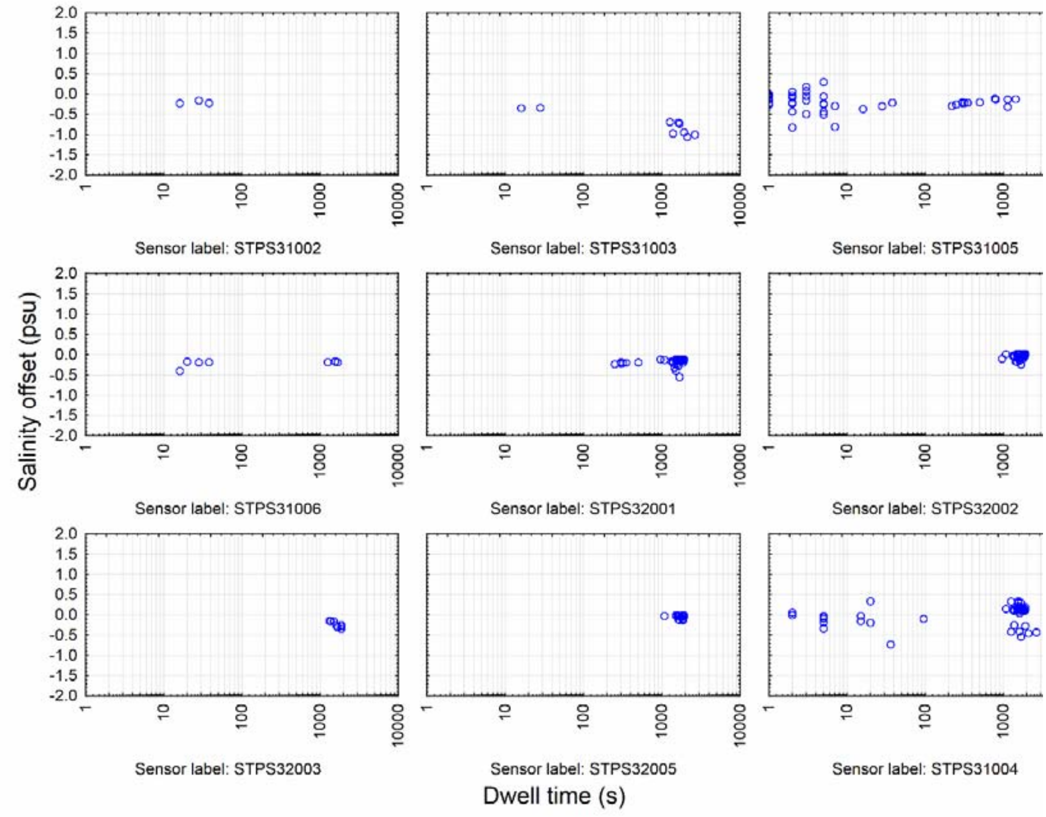

Figure 32. Salinity offset of the NKE sensors as a function of dwell time.

The correlation coefficient between the absolute value of the salinity offset and the temperature at the depth permanence of the NKE sensors is -0.09 which indicates a very weak association between the variables. In Fig.33, the salinity offset of each of the NKE sensors is plotted versus temperature at the depth permanence. An apparent decrease of the salinity offset with the increase of temperature is evident in most cases.

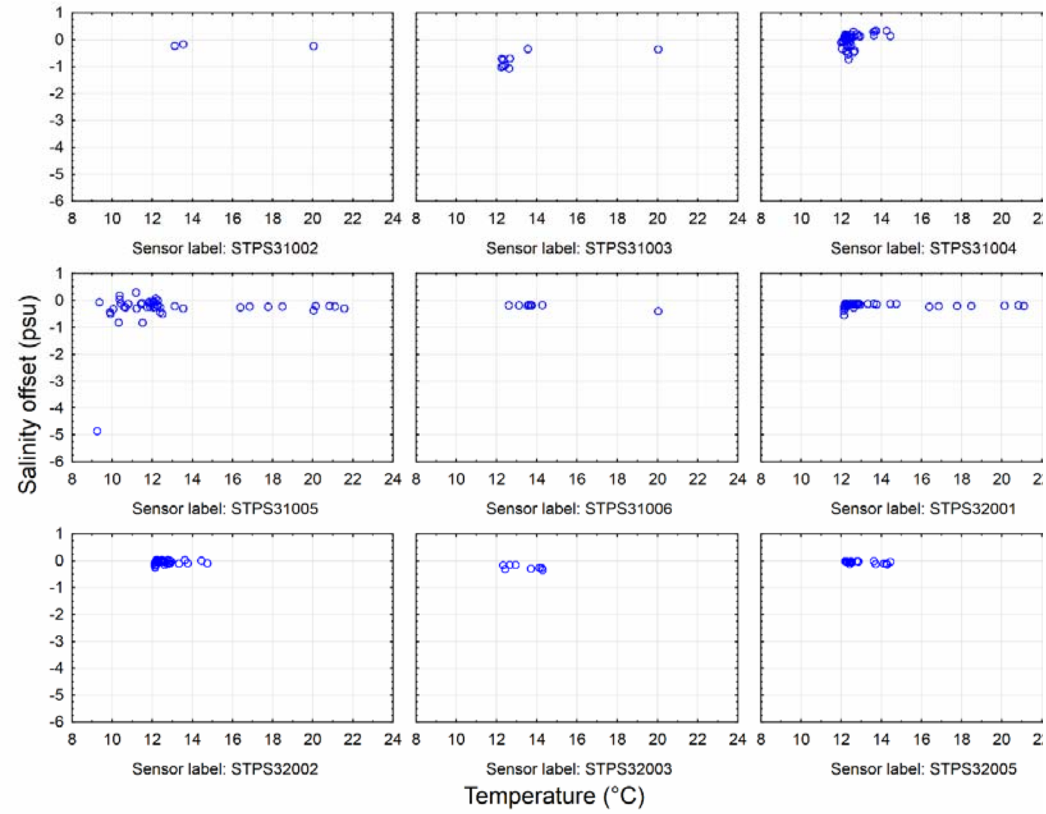

Figure 33. Salinity offset of the NKE sensors as a function of temperature at the depth permanence.

4.1.4. Scientific Results and conclusions

Several Star-Oddi sensors and NKE sensors, collectively indicated as FOS-FOOS sensors, were deployed together with a calibrated CTD SBE9/11plus instrument in occasion of different casts performed at different dates and different locations in the Adriatic sea. The purpose was to evaluate the offset between the reading of the FOS-FOOS sensor and the CTD reading regarding depth, temperature and salinity.

Due to the different time response of the sensors with respect to the CTD instrument, the offset between the FOS-FOOS sensors and the CTD instrument was calculated in correspondence of a depth permanence to avoid transient effects.

The Star-Oddi sensors have a depth offset which, in many cases, is larger than 2 m. In two cases, values higher than 7 m were also observed. The general offset is not depth-or time-dependent. The depth measurement of some sensors was not repeatable.

In most cases, the Star-Oddi sensors have a temperature offset in the range ±0.1°C, which is the nominal accuracy range of the sensor. However, several extreme offset values were also calculated. These extreme values have been shown to derive from a negative combination of the long time response of the temperature sensor and the short dwell time at the depth of the depth permanence. It was observed that in order to obtain a temperature reading according to the nominal accuracy, the dwell time should not be shorter than 50 s which is however longer than the nominal time response indicated by the manufacturer (20 s).

The NKE sensors have a depth offset which in most case is less than 1 m. Only for two sensors, the offset was larger than 2 m. No influence of depth or dwell time was observed on the depth offset.

The NKE sensors have a temperature offset which is in most cases inside the nominal accuracy range of the sensor (±0.05°C). Also in this case, however, the reading of the sensor is slightly time-dependent. When the dwell time of the NKE sensors was longer than 50s, almost all the offset values fall inside the nominal accuracy range of the sensor.

The NKE sensors have a salinity offset which in most of cases is outside the nominal accuracy range of the sensor. No influence of the depth or the dwell time was observed for the salinity offset. Moreover, the salinity reading of the NKE sensors is greatly influenced by the operating conditions, i.e. the water flow inside the sensor, which can cause a noisy reading. This noisy reading, when present, can be eliminated or greatly reduced by a post-processing of the raw data.

Summarizing the above results, it can be assessed that for oceanographic purposes, the data collected by Star-Oddi sensors are useful only considering the data portion where a dwell time at a fixed permanence is longer than 50 s. In this condition, the temperature offset is inside the nominal accuracy range of the sensor. Nor the descendent or ascendant part of a cast can be usefully corrected. Thus, when using them on a fishing gear, it is possible to be confident only in the dataset collected when the net/gear is actively fishing (which happens usually at a stable depth) and not during the deployment and recovery of the gear. The data collected by NKE sensors seem to be generally quite accurate both for depth and temperature, especially when the sensor is allowed to rest for more than 50 s. The weak point of the NKE sensors is the salinity measurement for which there seem to be no specific indication of operating conditions which could allow a better performance in particular for the offset which is in most cases outside the nominal accuracy of the sensors. The spiky salinity reading of the NKE sensor can be instead reduced by a simple post-processing of the raw data.

The offsets calculated by means of the above analyses will allow to correct (at least for the sensors here evaluated) the original values contained in the large dataset collected firstly by the FOS (from 2003 to 2013) and then by the FOOS (from 2014), thus making it more precise and reliable.

However the offsets here calculated were obtained in almost ideal conditions: all the sensors were rinsed with fresh water before any cast and their handling was definitely more “gentle” than those expected on a fishing ship. From this point of view, the performances of the FOS-FOOS sensors, in particular the conductivity ones, during fishing operations can be negatively affected, unfortunately in unpredictable way, by their cleaning conditions and handling.

Due to their very large response time, the data collected by the Star-Oddi sensors in the descendent or ascendant part of the casts cannot be corrected in any reliable way. In case of the NKE sensors, while considering the descendent or ascendant part of the casts, which correspond to the deployment and recovery of the fishing gear, besides the temperature offset, also the eventual depth inaccuracy of the sensor should be taken into account to obtain a reliable temperature-depth profile. In addition, during trials on the fishing gears, it was noticed that sometimes the NKE sensors need a longer stabilization period when entering the water if the air temperature is very different (e.g. after being left outside in strong sun irradiation conditions), thus the firsts given values should be considered carefully.

For what may concern the use of the conductivity data collected during the descent phase of the casts, it would be possible to correct them using a lowpass filter, and then applying the calculated offset, it would be possible to consider the data with the accuracy in salinity declared from the manufacturer. Even in this case, the performance of the sensor improves in stationary phase. In Appendix A, we have reported the median values of the depth, temperature and salinity offset of the tested sensors. The figures are rounded to the CTD accuracy (1 m for depth, 0.001°C for temperature and 0.02 for salinity). For the Star-Oddi sensors, the offsets are those calculated on casts with dwell time longer than 50 s, see text.

The authors of this report strongly suggest to other users, intended to use any kind of probes measuring oceanographic parameters for purpose similar to those here declared, to perform comparison analysis with CTD for every single probe before their usage, and then repeat them periodically.

In the near future, sensors able to collect more parameters (oxygen and chlorophyll-a fluorescence), designed specifically to be mounted on fishing gears and compatible with the systems in use nowadays (RECOPESCA, FOOS), will be available (Martinelli et al. 2014). Therefore, hopefully, the approach described in this report and developed in order to test sensors and moreover qualify the acquired data might be considered of interest for further developments.

4.1.5. Published Papers

Martinelli M., Campanelli A., Sparnocchia S., Paschini E., Waldmann C., Rolin J.F., Quemener L., Charria G., Delauney L., Malarde D., David A. Work Package 7 – Deliverable 7.2 – Preliminary studies and choice of new probes- FP7 Ocean 2013 NeXOS project “Next generation Low-Cost Multifunctional Web Enabled Ocean Sensor Systems Empowering Marine, Maritime and Fisheries Management”. 2014.

Martinelli M, Falco P, Belardinelli A, Cingolani N, Arneri E, Russo A, and Santojanni A. 2012. Fishery observing system (FOS): a tool for collecting oceanographic data and data on fish in the Adriatic. In: Operational Oceanography in Italy toward a sustainable management of the sea. ISBN: 978-88-87854-29-9, I Quaderni di Arpa: 277-284.

Martinelli M., Penna P., Belardinelli A., Croci C., Domenichetti F., Sparnocchia S., Santojanni A. From FOS to FOOS: Advances in use of fishing vessels for Oceanographical purpose in the Adriatic Sea. JERICO Workshop WP10. Villefranche/Mer, 16-18 Ottobre 2013.

5. Data Analysis Report on National Oceanographic Center FerryBox Data

The SNOMS Project (SWIRE NOCS Ocean Monitoring System) was borne of a ground breaking joint research project supported by the Swire Group Trust, the Swire Educational Trust, the China Navigation Company (CNCo) and the Natural Environment Research Council. The project was designed to gather high quality data on concentrations of carbon dioxide in the surface layer of the ocean. It has contributed to the international effort to better quantify (and understand the driving processes controlling) the exchanges of CO_2 between the ocean and the atmosphere. In 2006 and 2007 a system that could be used on a commercial ship to provide data over periods of several months with only limited maintenance by the ship's crew was designed and built by the National Oceanography Centre in Southampton (NOC). The system was fitted to the CNCo ship the MV Pacific Celebes in May 2007. During the period that the SNOMS system was installed the ship initially plied a circumglobal route, followed by a repeated trans-Pacific route. The data from the SNOMS project is archived at the British Oceanographic Data Centre (NOC; http://www.bodc.ac.uk) and the Carbon Dioxide Information and Advisory Center (CDIAC; Oak Ridge, USA; http://cdiac.ornl.gov/). Prior to its deployment on the Pacific Celebes, the system was run in tandem with an existing FerryBox system on the MV Pride of Bilbao and post deployment the complete system was sent to Halifax, Canada where its performance was assessed through testing at the Aquatron facility at Dalhousie University.

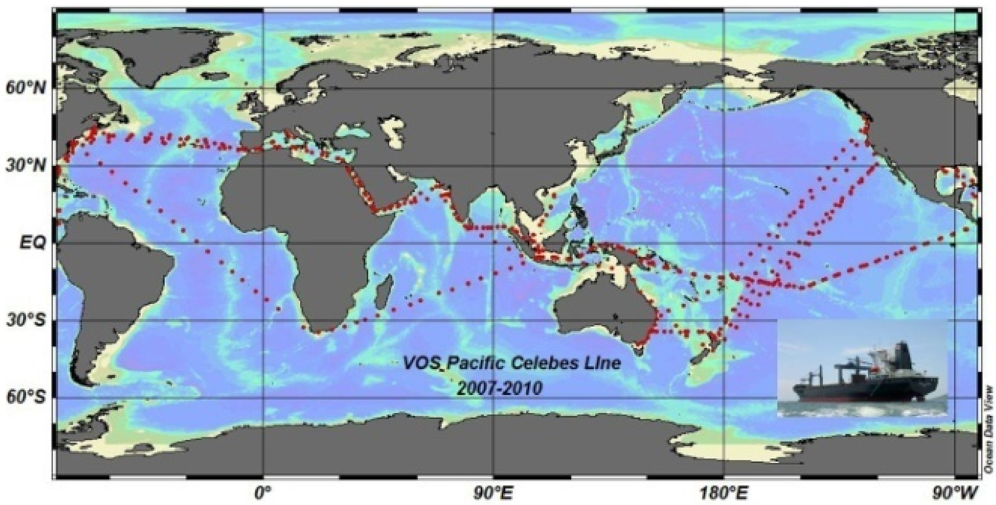

Figure 34 Track of vessel

5.1.1. Data collection methodology

Data collection were split into 3 types: 1) Continuous underway data from atmospheric and hydrological sensors was logged to a flash card and retrieved quarterly, 2) To monitor the operation of all the sensors in the system (listed in Table 1) a subset of the Continuous underway data (spot values at intervals of 5 minutes) were telemetered via an iridium satellite link to the NOC and displayed in near real-time on a public web-page at http://www.noc.soton.ac.uk/snoms and 3) discrete sample analysis based on daily samples which were collected and fixed by the ship's crew, collected quarterly, or more often, and analysed at NOC in the UK. The discrete sample positions are shown in the chart above; additionally, Figure 34 provides an overview of the data collection methods in the form of a flowchart.

Table 1. Sensor list

Manufacturer	Measurement	Model	Method	Serial numbers
Aanderaa	Sea water Temperature	4050	thermistor	11 13 15 25 34 55 90
Aanderaa	Sea water O_2concentration by Optode	3835	Fluorescence Quenching	338 339 340 641 34 1008 1009 1014 1357
Aanderaa	Sea water Conductivity	3919	Inductive	136 138 139 674 952 1C
Pro-Oceanus	Sea water CO_2 concentration	CO2-Pro	Infra Red absorption	47 48 94
Pro-Oceanus	Sea water dissolved gas fugacity	GTD-Pro	gas tension	49 98
SeaBird	Ship's Hull Temperature (in situ water)		Contact Thermistor	23 25
Vaisala	Atmospheric CO_2	GMP343	Infra Red absorption	B2840006 D4150004
Vaisala	Atmospheric pressure, temperature and humidity.	PTU-200	Press & Humidity –capacitive, temperature -PRT	
Vaisala	Atmospheric pressure, temperature and humidity.	PTU-300	Press & Humidity –capacitive, temperature -PRT	
Vector	Wind Direction	W200G	Vane	2118
Vector	Wind speed	A100R3	Cup anemometer	1894

5.1.2. Quality assurance applied

Hartman et al. (2012) describes the processing of the data that were written to flashcard storage. Two methods were used to provide quality control (QC) of the data sets:-

(1) In the case of the sensors providing data on tank temperature, conductivity and concentration of dissolved oxygen the measurements were replicated by using three of each type of sensor. The use of triplicate readings enabled the identification of less a well-functioning sensor. Following comparison of the match of the output from the three sensors a single output measurement based on the choice of the "best" most closely functioning instruments was generated. In addition a fourth a hull mounted temperature sensor provided a further cross check on the stability of the temperature measurements made in the tank and vice versa.

(2) Water samples (that are able to be stored without deteriorating for extended periods) were also collected, these provided quality control of the measurements of conductivity and the measurements of pCO2 (by calculation of pCO2 from measurements of Total Alkalinity - TA and Total Dissolved Inorganic Carbon - DIC made on the water sample). The ship's crew collected these seawater samples on a daily basis while the ship was underway. These consisted of a 200 ml salinity sample and a 250 ml sample for TA/DIC. The samples were shipped back to NOC for analysis from the break point ports in the operation, listed in Table 2. Hartman et al. (2012) describe the steps taken to achieve a "best" data set on a 5-minute time step. These were then adjusted as necessary on the basis of the water sample data. All,

adjustments made to the data and the precise scale of the adjustments are recorded in the meta-data set. A pictorial overview of the processing procedure is given in Figures 1 and 2 these should be used in conjunction with the written descriptions in Hartman et al (2012) to follow the procedures involved. The linked originating documents are publicly available from NOC.

For the Pro-CO2 Carbon Dioxide sensor, Table 2 provides an indication of the percentage of time data were considered of good enough quality to have the full set of quality control procedures applied.

Table 2 Break point ports for division of the data sets. If all equipment on board, (On – Yes or No). An indication to 10 % of the %age of time the main CO_2 sensor was collecting data to which quality controls could be applied.

Voyage	Start Port	End Port	Start date	On	CO_2 % good
1	Singapore	Livorno	02/06/07	Y	10 %
2	Livorno	Livorno	12/09/07	Y	20 %
3	Livorno	Livorno	29/01/08	Y	60 %
4	Livorno	St John	13/06/08	N	N
5	St John	St John	25/10/08	Y	100 %
6	St John	Livorno	21/03/09	Y	100 %
7	Livorno	Vancouver	18/08/09	Y	100 %
8	Vancouver	Vancouver	27/11/09	Y	50 %
9	Vancouver	Vancouver	21/03/10	Y	100 %
10	Vancouver	Vancouver	23/06/10	Y	40 %
11	Vancouver	Vancouver	28/09/10	Y	100 %
12	Vancouver	Vancouver	14/01/11	N	N
13	Vancouver	Vancouver	29/04/11	Y	90 %
14	Vancouver	Vancouver	26/07/11	Y	100 %
15	Vancouver	Vancouver	29/10/11	Y	100 %
16	Vancouver	Melbourne	05/02/12	Y	100 %

A spreadsheet is presented in Annex 6 of Hydes et al., (2013) that provides details the times data from each of the sensors used passed the initial visual inspection stage.

The basic steps described in detail in Hartman et al. (2012) are:-

(1) After the data had been transferred from the flashcards they were processed using bespoke NOC software coded in the C-language-code using Lab VIEW™ software. This software concatenates, averages and merges the parameters from all of the instruments and converts the binary files into ASCII files for further processing.

(2) Further processing of the data was performed using procedures that were coded using MathWorks Inc's Matlab™ software to inspect, quality control, adjust and write the archive-able data files, figure 35 shows a flowchart example of the main processing stages and notes the importance of providing a continuous record of meta data to accompany the data through the processing stages.

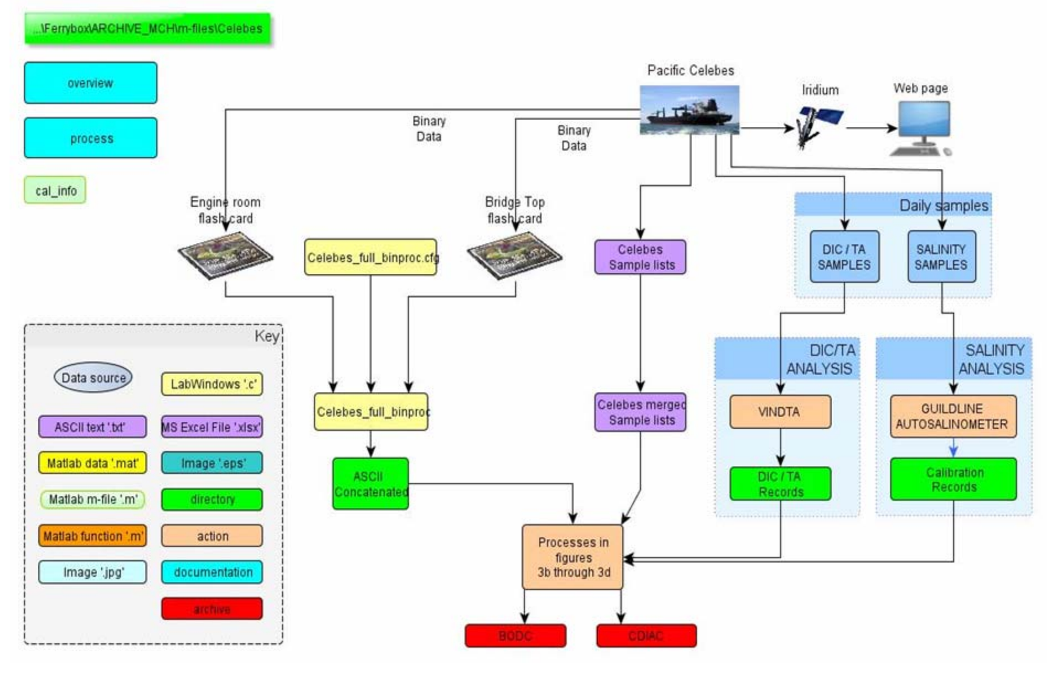

Figure 35 Data and samples transferred from M.V. Pacific Celebes to NOC

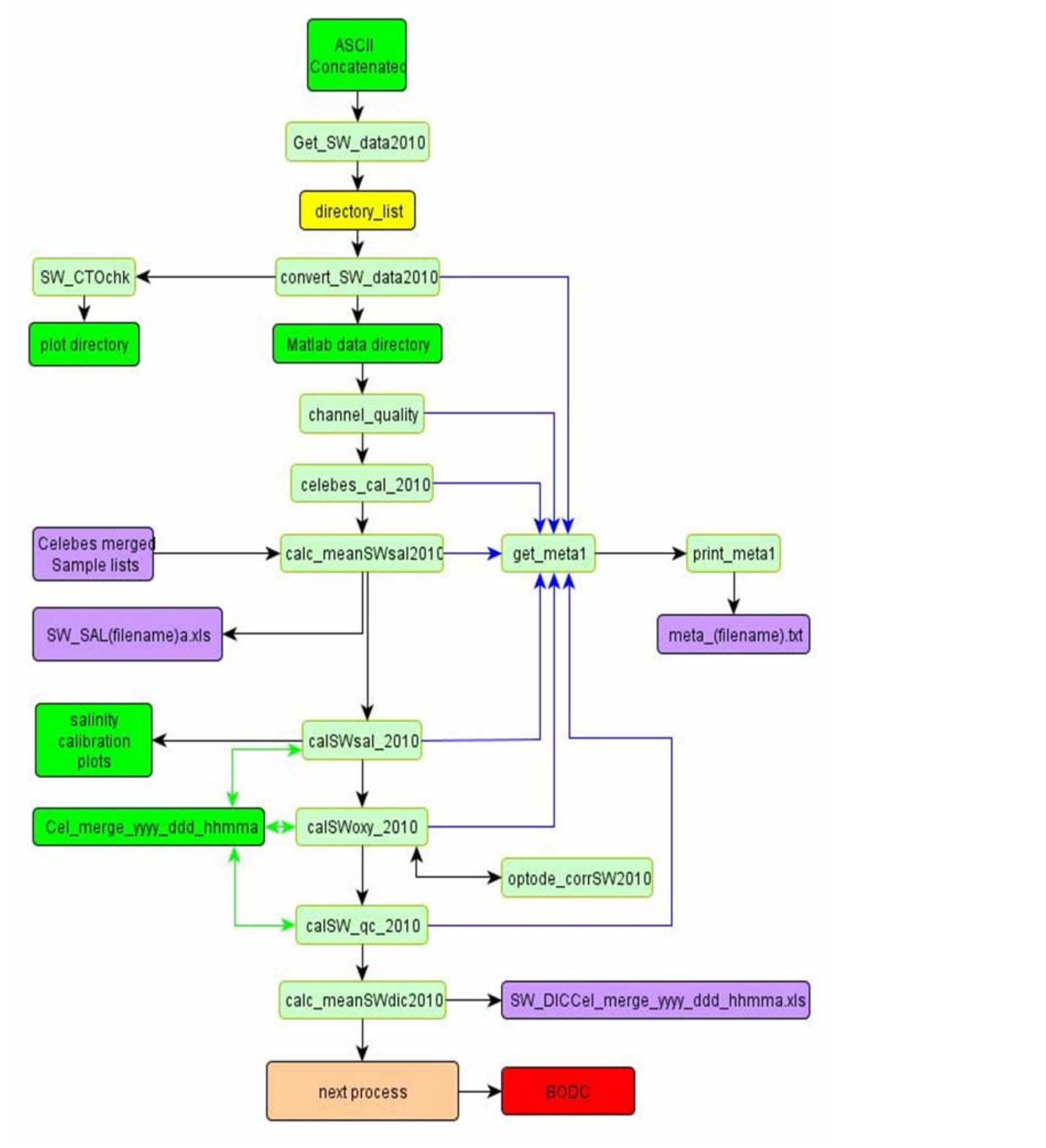

Figure 16 Underway Data processing

5.1.3. Analysis

The two types of discrete samples collected provided information on 1) salinity; measured using a high precision Guildline Autosal™ salinometer in a temperature controlled laboratory referenced to IAPSO standard seawater and 2) on the Dissolved Inorganic Carbon (DIC) content and the Total Alkalinity (TA) of the sea water, measured using Marianda VINDTA-3C™ instrument; these measurements are standardised by measuring certificated reference solutions alongside the samples.

5.1.4. Scientific results

As well as contributing to the global coverage of surface CO_2 measurements, the results from the study have yielded insight into the relationship between salinity and alkalinity; they have also given insight into the quality of the data that it is possible to obtain from extended unattended observations using membrane based CO_2 sensing technology. Additionally, the calculation of dissolved nitrogen enables changes in gas saturation due to physical and biological processes to be separated.

5.1.5. Published papers

Variability of alkalinity and the alkalinity-salinity relationship in the tropical and subtropical surface ocean. Zong-Pei Jiang, Toby Tyrrell, David J. Hydes, Minhan Dai, Susan E. Hartman, Global Biogeochemical Cycles, Volume 28, Issue 7, pages 729–742, July 2014 DOI: 10.1002/2013GB004678

Jiang, Zong-Pei; Hydes, David J.; Hartman, Sue E.; Hartman, Mark C.; Campbell, Jon M.; Johnson, Bruce D.; Schofield, Bryan; Turk, Daniela; Wallace, Douglas; Burt, William; Thomas, Helmuth; Cosca, Cathy; Feely, Richard. (2014) Application and assessment of a membrane-based pCO2 sensor under field and laboratory conditions. Limnology and Oceanography: Methods, 12. 264-280. 10.4319/lom.2014.12.264

M C Hartman, D J Hydes, J M Campbell, Z P Jiang & S E Hartman (2012). Data processing procedures for SNOMS project 2007 to 2012 Version-1: 28 August 2012. Soton eprints Internal Document No. 05. http://eprints.soton.ac.uk/342198/

Hydes, D.J., Hartman, M.C., Campbell, J.M., Jiang, Z-P., Hartman, S.E., Pagnani, M., Kelly-Gerreyn, B.A. and Donahoe, J. (2013) Report of the SNOMS Project 2006 to 2012, SNOMS SWIRE NOCS Ocean Monitoring System. Part 1: Narrative description. Southampton, UK, National Oceanography Centre, 40pp.(National Oceanography Centre Research and Consultancy Report, 33). http://eprints.soton.ac.uk/350263/

DJ Hydes PhD, MC Hartman BSc, CP Bargeron MSc, JM Campbell MSc, MS Cure´ PhD, DK Woolf PhD, (2008) "A study of gas exchange during the transition from deep winter mixing to spring bloom in the Bay of Biscay measured by continuous observation from a ship of opportunity." Journal of Operational Oceanography 1(2): 41-50.

6. Real-time quality control (RTQC) overview

Given the importance of the coastal seas to the European economy and to the communities living on its coastlines, knowing the state of the coastal ocean is vital. One way to capture the state of the ocean is constantly monitoring the main hydrographic variables. For this task, the FerryBox system is a valuable tool.

The FerryBox concept has been developed in partnership with scientists and with companies that operate ferries in Europe. Similar activities started around the world (Hydes et al., 2010). Meanwhile, not only ferries, but also cargo ships are used.

In general, all FerryBox systems employ a similar design. There are differences in the design of the flow-through system, the degree of automation and biofouling prevention as well as the possibilities of supervision and remote control. The concept was tested intensively in the EU FP5 project "FerryBox" (2002–2005). In this project, at least four "core" sensors for temperature, salinity, chlorophyll fluorescence and turbidity were operated by all the partners (Petersen et al., 2007). Presently in Europe, approximately thirty ships are involved in this type of work (www.ferrybox.org). In Figure an overview of the present FerryBox lines in European coastal waters are shown.

There are numerous advantages to the FerryBox system: no ship costs, no energy restrictions, regular maintenance is possible, transects are sampled repeatedly and problems with biofouling of sensors can be better controlled. There is great potential for data coverage using ferries and cargo ships cruising the same route on a regular basis, especially in coastal regions.

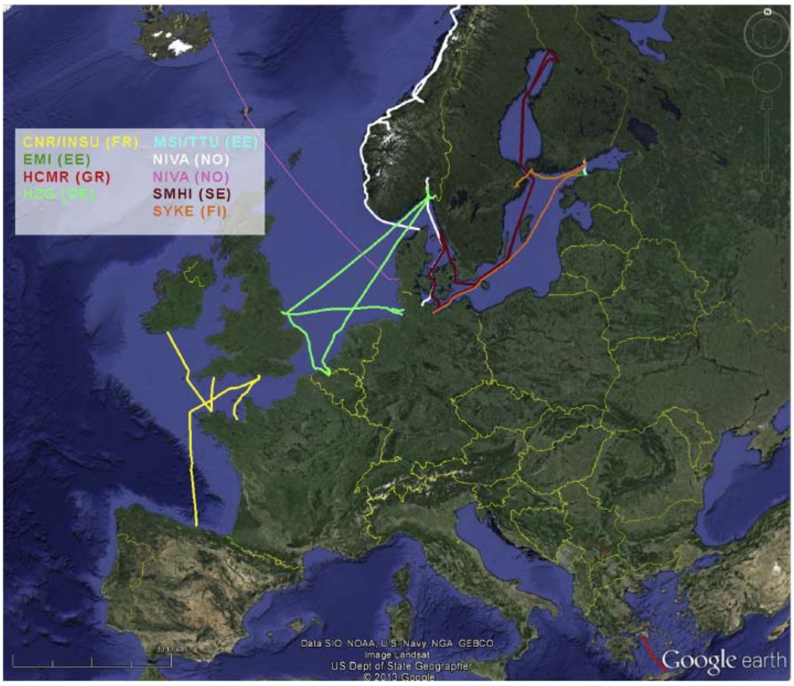

Figure 37 : FerryBox lines in European coastal waters at present (from Petersen (2014)).

However, continuous operation of FerryBox lines creates a large volume of data and requires appropriate data management. A reliable quality assessment is mandatory. Within the European project MyOcean (www.myocean.eu), a subset of most of the FerryBox data within Europe (temperature, salinity, chlorophyll-a fluorescence) is delivered to NIVA, undergoes distinct automatic quality checks and is available as netCDF files from the MyOcean FTP server.

This report addresses the challenge of real-time quality control, which should be performed on board of the FerryBox systems and in the data bases of the FerryBox operators. It was enquired which tests are performed and examples of the data quality flow will be shown.

With the development of operational oceanography observing systems, the need for real time data quality control became essential. The task of joined European observing systems has been since then to standardize and harmonize the procedures of quality control in (near) real time. Real time in this context means a time range of hours to a week at maximum (Pouliquen, 2010). For a standardized procedure, recommendations have been formulated for physical parameters by the EuroGOOS working group “Data Management, Exchange and Quality” (DATA-MEQ, http://www.eurogoos.org). Involved were also institutions like SeaDataNet and EU projects such as FerryBox, MyOcean, Mersea etc. The recommendations have been brought together in Pouliquen (2010) and will be summarized here for FerryBox systems.

Real time quality controls (RTQC) for FerryBoxes are based on those for time series in general; however, there are some specialties that are valid only for FerryBoxes. In Table 3 the FerryBox specific quality tests are summarized. The tests that are valid for all platforms are

- Platform meta data test

- Impossible date test
- Impossible location test
- Global/regional test.

Test type	Description
Frozen date/location/speed test	This test is a check if the navigation system is updating.
Speed range test	This tests checks whether the given speed is inside the threshold values for minimum and maximum speed. Some FerryBoxes are turned off in harbour.
Pump of flow-meter test	The state of the pump should be tested, or alternatively a test of the flow-rate measured by the flow-meter, when available on the FerryBox system, should be performed.
Pump history test	The pump should be working during a minimal period after it has been stopped in order to make sure water in the system has been renewed. The correct threshold value will depend on the pump capacity and system design.
Gradient test	Horizontal gradient tests must take into account the distance between adjacent measurements. This will depend on ship speed and data logging frequency. Moreover, only adjacent data measured at expected intervals should be taken into account in the test. This test includes testing of spikes. Threshold values are likely to depend very much on regional specifications.
Spike test	A spike is a point in the data series which has an anomalous value outside of the surrounding range. This algorithm is used on the current speeds: Test value = $\lvert V2 - (V3 + V1) / 2 \rvert - \lvert (V3 - V1) / 2 \rvert$, where V2 is the measurement being tested as a spike, and V1 and V3 are the values above and below.
Variance test	If variance is available calculated from averaging measurements over a certain time period it can be used as a criteria to remove noisy data (e.g. caused by air bubbles) as well as frozen values.

Table 3 : Summary of FerryBox specific real time quality control (RTQC) tests (adapted from Pouliquen (2010)).

6.1. Survey of RTQC checks performed by JERICO partners

For an overview of the RTQC checks that are applied in the European FerryBox community, a survey has been conducted among the partners. A list of tests generated from Table 3 and the general tests has been distributed among the partners for clarifying which tests are applied. The results are shown in Table.

The FerryBox data of **HCMR** are processed in real-time by FerryBox software on board in terms of testing location, pump history and date. Then the data are transmitted to Poseidon system data centre after each transect and all the additional tests are performed in the data base.

For the **INSU-MIO** data, all quality tests are performed except the variance test. In these cases, no FerryBox system are used but low-cost but fully autonomous thermosalinometer systems (~15k€ total) that are extremely reliable. For the pump of flow-meter test, the difference between the hull/SST from SBE38 and the temperature from SBE45 is used instead (marked in Table 4 as A). The circuit is very short, and the median computed is ~0.2°C. The test is done following: any value <0 is doubtful and removed; any value above and below a threshold (defined for every ship) is removed. So any value inside the range means that the pump is working properly.

The regional test (marked in Table 4 as B) has been adjusted due to the large variations between North and South of the Mediterranean, and to the large variability in time and in space due to upwellings, river plumes etc. So is has been implemented in a way that the regional range tests are coupled with seasonal range tests.

The gradient test is not relevant for INSU-MIO FerryBox data due to the large variability and, thus, is not implemented.

At **SYKE and SMHI**, the impossible date and location tests are performed as well as the pump or flow-meter test (only SYKE) and the global/regional tests.

Commentaire [MH1] : Bengt, could you please check if the SMHI description is correct ? Same for the table below

The **HZG** data quality checks consist of the frozen date/location/speed test for their FerryBox data. Furthermore, the global/regional tests and the variance tests are performed. At denoted in the table, spike tests and gradient tests are performed only for fixed FerryBox platforms, i.e. at Cuxhaven harbour site and FINO3 platform.

IFREMER

In general, the highest agreement consists in the application of regional and global tests. They are performed by all partners. Most institutes use either the impossible tests or the frozen tests. The tests concerning the pump reliability are applied by a majority of institutes.

The group of spike, gradient and variance tests is not commonly used but only by a few institutes. Maybe this could be a matter of improvement for harmonization of data quality control on European level.

RTQC for FerryBoxes	HZG	NIVA	SMHI	SYKE	HCMR	INSU-MIO	Ifremer
Platform metadata check					x[1]	x	
impossible date test			x	x	x	x	
impossible location test			x	x	x	x	
Frozen date/location/speed test	x	x			x[1]	x	
Speed range test		x			x[1]	x	
Pump or flow-meter test	x	x		x	x[1]	A	
Pump history test	x				x	x	

Global range test	x	x	x	x	x[1]	x	
Regional range test	x	x	x	x	x[1]	B	
Gradient test	x[2]	x			x[1]	C	
Spike test	x[2]	x				x	
Variance test	x						

Table 4 : Survey of applied RTQC tests among JERICO partners operating FerryBox systems. [1]Test is done by Poseidon system data centre. Specifications for INSU-MIO are outlined in the text. [2]Tests are only done for fixed FerryBox platform data (e.g. at Cuxhaven harbour site).

6.2. Examples of RTQC check procedures

6.2.1. Quality controls in MyOcean

MyOcean is the implementation project of the GMES Marine Core Service (Copernicus), aiming at deploying the first concerted and integrated pan-European capacity for Ocean Monitoring and Forecasting http://www.myocean.eu.org). In MyOcean data from approximately 20 FerryBox systems has been handled and send to the MyOcean operational QA-systems. This can be directly from the ship or through the national operation (server) after some pre-QA procedures (see Figure). An important step within MyOcean is to harmonize and further develop the existing Real Time Quality Control (RTQC) and quality assurance procedures of the different areas involved.

One of the various tasks of the MyOcean project deals with the scientific and technical validation of In Situ-TAC (Technical Assembly Centres) products and forms the frame of this document. WP15 aims to perform operational quality control (QC) of global and regional products as well as to lead scientific assessment validation activities with regional responsibilities. Beside global scale products, regional specifications are performed in the Arctic, the Black Sea, the North- western Shelves, the Baltic Sea, the South-western Shelves and the Mediterranean Sea. It follows therewith the EuroGOOS regional approach, with establishing regional alliances.

The MyOcean quality tests procedures are distinguished between temperature/salinity data and biogeochemical data.

The quality controlled database is freely shared and used for various applications in the marine environment. Thus, after the RTQC procedure, an extensive use of flags to indicate the data quality is vital since the end user will permit the selection of the data based on quality flags amongst other criteria. These flags need always to be included with any data transfer that takes place to maintain standards and to ensure data consistency and reliability.

For the QC flags for temperature and salinity within MyOcean an extended scheme is generally proposed and applied for MyOcean (Table).

At present the use of nutrient sensors on autonomous platforms is very limited (D'Ortenzio et al., 2010). The amount of nutrient data delivered to MyOcean in real time was very low. The quality tests are therefore defined for Chlorophyll a (Chl-a) fluorescence and oxygen measurements only.

When using real-time measurements of Chl-a fluorescence as a proxy for Chl-a concentration, the users should be aware of the natural variation in Chl-a fluorescence relative to Chl-a concentration. Thus, there is a need to clearly distinct between bad Chl-a fluorescence data caused by sensor failure or bad calibration and "uncertain" estimates of Chl-a concentration caused by inherent natural variations in the Chl-a fluorescence.

The detection of anomalous values of BGC parameters is challenging due to their inherent high spatial and temporal variability, e.g. diel Chl-a fluorescence can vary with as much as a factor 4, and can change as a result of cloud cover (Huot and Babin, 2010). It is therefore a challenge to define regional tests to check data quality in sea regions having different characteristics.

Some of the automated QC procedures in MyOcean have been derived from those developed for the QC of Argo data management (ARGO, 2009).
Formulations for the QC tests on Chl-a data have also been adopted from the PABIM white book (D'Ortenzio et al., 2010). To improve the efficiency of some tests, specifications are incorporated into the validation process of regional measurements, depending on local water mass structures, statistics of data anomalies, as well as using regional enhanced bathymetry.
It should be stressed out that some BGC parameters cannot be thoroughly quality controlled without knowledge of the sensor, the way it was calibrated and even when it was used.

MyOcean does only cover data management but it is out of the scope of the project to establish best practice.

Most of the ARGO QC RT tests are performed to identify problems related to bad geo-localization, erroneous timing, wrong platform identification, pressure errors etc. For these tests, the ARGO procedure is strictly adopted also for the RTQC on BGC data.

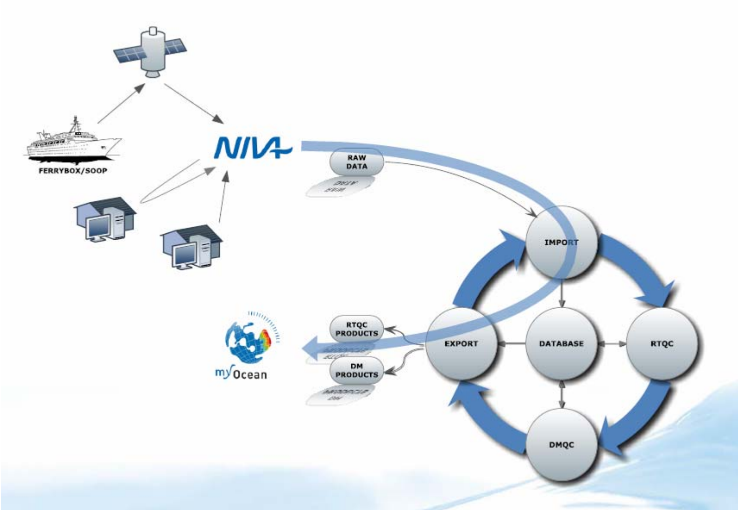

Figure 38 : FerryBox data flow at MyOcean and NIVA.

Code	Meaning
0	No QC was performed
1	Good data
2	Probably good data
3	Bad data that are potentially correctable
4	Bad data
5	Value changed
6	Below detection limit
7	In excess of quoted value

8	Interpolated value
9	Missing value
A	Incomplete information

Table 5 : Quality flag scales in MyOcean. Flags marked in red are mandatory following the RTQC procedures.

6.2.2. Quality control procedure at HZG

At HZG all data are stored on board first. Figure 38 shows the data flow from the vessel to the database on shore. The data are transmitted to the shore either via mobile phone connection (GSM or UMTS) or satellite communication after finalizing the transect and when the ship has reached the harbour.
Before transfer, the FerryBox data are quality checked and flagged in real-time according to above described recommendations for near real-time quality control of the EuroGOOS working group DATA-MEQ. Among other issues, these quality checks deal with frozen values, spikes, as well as flow rates within the flow-through system, or the speed of the ship. The data are stored in a relational database (http://ferrydata.hzg.de) which is embedded in the data portal of the coastal observatory COSYNA (www.cosyna.de), where the FerryBox data can be additionally combined and compared with data from other sources (Breitbach et al., 2010). Furthermore, a manual tool is available where flagging could be done after the real-time quality control. An overview is given in the Annexes.

The free web-based online database has several tools for data visualization as well as data download. For example, all data along a single transect can be plotted against distance (both latitude and longitude alternatively), or all data at a certain position can be plotted over a specific period of time as a time-series. Another option provided is the ability to pool all data along a transect over a selected time period and plot the physical values coded as colour levels in a time/distance diagram in order to show the temporal variability of a particular parameter along the transect. Furthermore, the coded colour levels of one selected parameter along a transect can be exported as a kml-file and directly visualized in Google™ Earth with overlays of other data, such as a satellite images of chlorophyll-a.

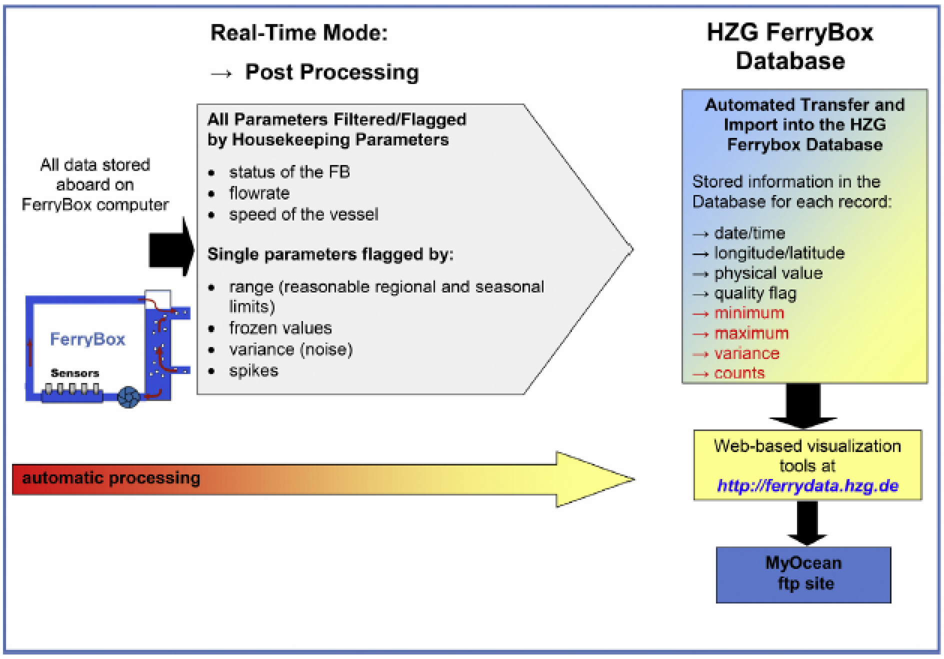

Figure 29 : Scheme of real-time post processing of FerryBox data from HZG.

Id	FB	FB Description	RGB
1	-1	bad data	
2	0	raw data no check	
3	1	raw data, range checked automatically by reasonable regional and seasonal limits	
4	2	raw data, automatic check procedures applied (range, flow, speed, variance etc)	
5	3	raw data, range checked automatically and manually removed spikes by visual control	
6	4	usable data, but doubtful calibration	
7	5	not yet defined	
8	6	probably good data, QC data (reference samples or calibration data) not available	
9	7	best estimate of recalibrated data	
10	8	quality controlled data (quality control by validation and calibration)	

Table 6 : List of quality flags for FerryBox data at HZG.

6.2.3. *Quality control procedures at SMHI*

Data from automated measurements should be sent to an oceanographic data centre in near real time if feasible.

The raw data (QC level 0) should be stored without modifications. The first step in the QC-process should be carried out automatically using algorithms to remove out of range data etc. to reach QC level 1 MyOcean has described this process in some detail. Scripts for carrying out this has been developed by several institutes and code is available e.g. in the Python programming language (open source) and in MatLab™ (Mathworks Inc.). The QC1-level data should be made freely available to the oceanographic community in near real time.

The next step in the QC process (QC level 2) is to compare the automated measurements with data from reference measurements (water samples analysed in an oceanographic laboratory) and with historical data from the same geographic area and season. This is conveniently made with the same interval as the service interval of the FerryBox-system in question, often every week or every two weeks. A semi-automated system for this may be developed using different databases and scripting software. SMHI has developed an open source solution, named *FerryBox Tools*, to make the process efficient. It has a user friendly interface adapted for non-programmers, based on Python scripts that collects data from databases, produces graphs and maps of the data.

The data is flagged according to MyOcean standards. Problems noted, e.g. bio-fouling of sensors etc. may now quickly be rectified during the next service visit to the ship with the FerryBox system.

The last step in the QC process to reach QC level 3 is carried out yearly when the whole data set for the year is plotted and compared to reference samples and historical data. FerryBox *Tools* is useful also for this. The QC3-level data should be made freely available to the oceanographic community for long term use.

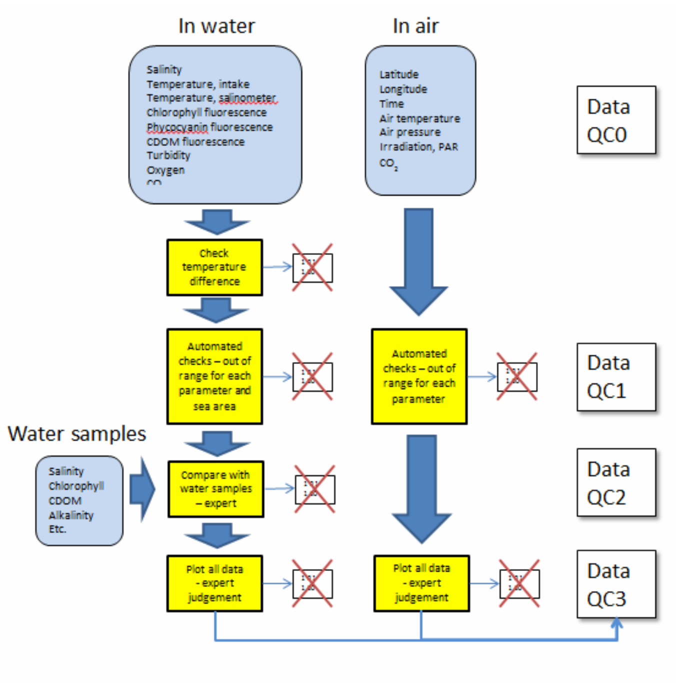

Figure 31 : Scheme of quality control of FerryBox data at SMHI.

6.2.4. Quality control procedures at NERC/NOC

Hartman et al. (2012) describes the processing of the data that were written to flashcard storage. Two methods were used to provide quality control (QC) of the data sets:

- In the case of the sensors providing data on tank temperature, conductivity and concentration of dissolved oxygen the measurements were replicated by using three of each type of sensor. The use of triplicate readings enabled the identification of less a well-functioning sensor. Following comparison of the match of the output from the three sensors a single output measurement based on the choice of the “best” most closely functioning instruments was generated. In addition a fourth a hull mounted temperature sensor provided a further cross check on the stability of the temperature measurements made in the tank and vice versa.

- Water samples (that are able to be stored without deteriorating for extended periods) were also collected, these provided quality control of the measurements of conductivity and the measurements of pCO2 (by calculation of pCO2 from measurements of Total Alkalinity - TA and Total Dissolved Inorganic Carbon - DIC made on the water sample). The ship’s crew collected these seawater samples on a daily basis while the ship was underway. These consisted of a 200 ml salinity sample and a 250 ml sample for TA/DIC. The samples were shipped back to NOC for analysis from the break point ports in the operation. Hartman et al. (2012) describe the steps taken to achieve a "best" data set on a 5-minute time step. These were then adjusted as necessary on the basis of the water sample data. All, adjustments made to the data and the precise scale of the adjustments are recorded in the meta-data set. A pictorial overview of the processing procedure is given in Figure .. The originating documents are publicly available from NOC.

A spreadsheet is presented in Annex 6 of Hydes et al. (2013) that provides details the times data from each of the sensors used passed the initial visual inspection stage.

The basic steps described in detail in Hartman et al. (2012) are:-

(3) After the data had been transferred from the flashcards they were processed using bespoke NOC software coded in the C-language-code using Lab VIEW™ software. This software concatenates, averages and merges the parameters from all of the instruments and converts the binary files into ASCII files for further processing.

(4) Further processing of the data was performed using procedures that were coded using MathWorks Inc. Matlab™ software to inspect, quality control, adjust and write the archive-able data files.

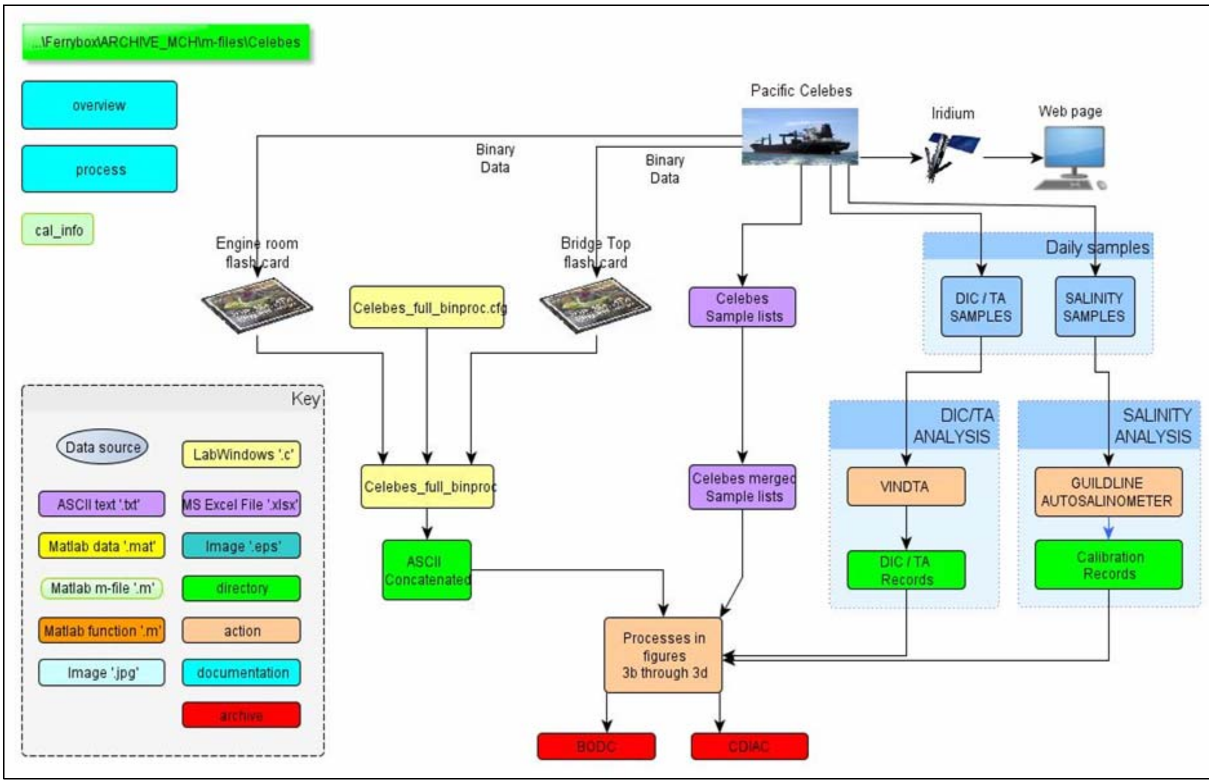

Figure 42: Data and samples transferred from M.V. Pacific Celebes to NOC.

6.3. Conclusions

It is agreed in the European community of ocean monitoring institutes that a detailed real-time quality control is mandatory for reliable data.

Real time quality controls (RTQC) procedures have been formulated, e.g. in ARGO (2009). For all kinds of platform there are general tests applicable as follows:

- Platform meta data test
- Impossible date test
- Impossible location test
- Global/regional test.

They are thus also usable for FerryBoxes; however, there are some specialties that are valid only for FerryBoxes which have been summarized in Table 6 .

A survey among JERICO partners showed that quality control tests are widely accepted and adopted. However, it revealed also that the application of the tests is not entirely consistent in the community. This has several reasons:

- There are different systems used, e.g. varying FerryBox version, simpler systems etc.
- Different philosophies
- Different regions and different according demands (e.g. salinity range)

The data processing process is often split up in parts that are done directly on board and parts that are performed at the data base at land. The second part is done in some cases by central data centres (MyOcean, Poseidon).

The delayed mode quality control is more complex and time demanding than the real-time quality control. For the delayed mode, sampling of water probes is an important task. Water samples should be analysed as quickly as possible. Validation protocols compare the results of certain sensors installed on a FerryBox system to bottle samples taken during the ship passage (salinity, turbidity, chlorophyll-a, nutrients) by a cooled automated water sampler or manually in the harbour (oxygen, total alkalinity, inorganic carbon).

Automation of delayed mode quality control is much more difficult than the real-time mode. First attempts of semi-automated data quality control are done by e.g. SMHI, HZG and NOCS. However, expert judgement is still needed for these steps. In the Annexes, two examples of a delayed semi-automated data quality control are shown.

7. Profiling technology inter-comparison with mature buoy technology Report

7.1. Introduction

An experiment was planned to use a tethered mooring ARVOR-C profiling float alongside the MAMBO buoy in the Northern Adriatic and compare with ship based CTD systems.

The tethering frame bearing the ARVOR-C float was to be moored close to the chosen Mambo profiling buoy - the float was to be programmed to profile once an hour so as to be able to provide data in concomitance with the transmissions of the profiles from the buoy which took place every three hours. The data from the two systems were to be supplemented with those from intermittent CTD casts that were to be carried out whenever possible during the period of the deployment.

The float with its frame was deployed on 07 November 2013. The float broke free on 15 November under very bad weather conditions, and was recovered. The frame was found to be intact but the supporting wire had snapped, and the fastening mechanism was broken. The mechanism was repaired and the wire was replaced with a stronger one. Other small structural modifications were carried out to render the whole system more robust. The profiles made by the float during its time at sea were downloaded. Subsequently, the unit was re-programmed and re-deployed on 10 January 2014 despite the continuing bad weather. On 17 January, the same thing happened again. This time, the float was recovered and sent back to IFREMER after downloading all its stored data. The buoy controller had failed, too, for some reason, during both periods, **so no buoy profiles were available for comparison**. Notwithstanding the several setbacks, the trial can be considered a partial success. When the float was operational, it did profile regularly, holding its position. It is clear that the tethering frame needs more work, in terms of both the design as well as the kinds of materials that were used, in order to make it able to weather really harsh sea conditions. The information gathered during the sea trial that was performed has provided valuable insights on the nature of the problems to be faced, and has helped to formulate new ideas for the further development of the system – however there is no data of sufficient quality collected during the deployment to run an inter-comparison. A full Report on this trial can be viewed in Work Package 10 Deliverable 10.1.

7.1.1. Results

While the field experiments outlined in the deliverable provide an inter-comparison between key oceanographic measurements carried out using different platforms – there is a distinct technical challenge remaining in ruggedizing/modifying existing winch technology to cope with open ocean conditions widely experienced in the Atlantic, Arctic Oceans and the Mediterranean Sea.

8. References

ARGO: ARGO quality control management., ARGO data management, 2009.

Breitbach, G., Krasemann, H., and Onken, R.: Data Management in COSYNA - COastal Observing System for Northern and Arctic Seas, University of Cologne, 29-30 October 2009 2010, 19-25.

D'Ortenzio, F., Thierry, V., Eldin, G., Claustre, H., Testor, P., Coatanoan, C., Tedetti, M., Giunet, C., Poteau, A., Prieur, L., Lefevre, M., Bourrin, F., Carval, T., Goutx, M., Garcon, V., Thouron, D., Lacombe, M., Lherminier, P., Loisiel, H., Mortier, L., and Antoine, D.: White Book on Oceanic Autonomous Platforms for Biogeochemical Studies: Instrumentation and Measure., 2010.

Hartman, M. C., Hydes, D. J., Campbell, J. M., Jiang, Z. P., and Hartman, S. E.: Data processing procedures for SNOMS project 2007 to 2012. Version-1, Southampton, UK, 51 pp., 2012.

Huot, Y. and Babin, M.: Overview of fluorescence protocols: Theory, basic concepts, and practice. Chap. 3, Springer, Berlin, 2010.

Hydes, D.J., Hartman, M.C., Campbell, J.M., Jiang, Z-P., Hartman, S.E., Pagnani, M., Kelly-Gerreyn, B.A. and Donahoe, J. (2013) Report of the SNOMS Project 2006 to 2012, SNOMS SWIRE NOCS Ocean Monitoring System. Part 1: Narrative description. Southampton, UK, National Oceanography Centre, 40pp.National Oceanography Centre Research andConsultancyReport (, 33). http://eprints.soton.ac.uk/350263/

Hydes, D. J., B.A. Kelly-Gerreyn, B. A., Colijn, F., Petersen, W., Schroeder, F., Mills, D. K., Durand, D., Wehde, H., Sorensen, K., and Morrison, G.: The way forward in developing and integrating FerryBox technologies., Venice, Italy, 21-25 September 2009 2010.

Hydes D.J. PhD, MC Hartman BSc, CP Bargeron MSc, JM Campbell MSc, MS Cure´ PhD, DK Woolf PhD, (2008) "A study of gas exchange during the transition from deep winter mixing to spring bloom in the Bay of Biscay measured by continuous observation from a ship of opportunity." Journal of Operational Oceanography 1(2): 41-50.

Hydes, D. J., Hartman, M. C., Campbell, J. M., Jiang, Z. P., Hartman, S. E., Pagnani, M., Kelly-Gerreyn, B. A., and Donahoe, J.: Report of the SNOMS Project 2006 to 2012, SNOMS SWIRE NOCS Ocean Monitoring System. Part 2: Detailed Technical and Data Annexes. National Oceanography Centre Research and Consultancy Report, 34, National Oceanography Centre Southampton, Southampton, UK, 2013.

Jiang, Zong-Pei; Hydes, David J.; Hartman, Sue E.; Hartman, Mark C.; Campbell, Jon M.; Johnson, Bruce D.; Schofield, Bryan; Turk, Daniela; Wallace, Douglas; Burt, William; Thomas, Helmuth; Cosca, Cathy; Feely, Richard. (2014) Application and assessment of a membrane-based pCO2 sensor under field and laboratory conditions. Limnology and Oceanography: Methods, 12. 264-280. 10.4319/lom.2014.12.264

Petersen, W.: FerryBox systems: State-of-the-art in Europe and future development, Journal of Marine Systems, 140, Part A, 4-12, 2014.

Petersen, W., Colijn, F., Hydes, D. J., and Schroeder, F.: FerryBox: From on-line oceanographic observations to environmental information. EU Project FerryBox 2002-2005, EuroGOOS Publications, 25, 36, 2007.

Pouliquen, S.: Recommendations for in-situ data Near Real Time Quality Control, 2010.

Zong-Pei Jiang, Toby Tyrrell, David J. Hydes, Minhan Dai, Susan E. Hartman, Global Biogeochemical Cycles, Volume 28, Issue 7, pages 729–742, July 2014 DOI: 10.1002/2013GB004678 - Variability of alkalinity and the alkalinity-salinity relationship in the tropical and subtropical surface ocean.

9. APPENDIX

9.1. Depth and temperature offset of the Star-Oddi sensors

Table 7. Median value of depth and temperature offset of the Star-Oddi sensors for cast with a dwell time at the depth permanence larger than 50 s. The figures are rounded to the CTD accuracy.

SENSOR LABEL	DEPTH OFFSET (m)	TEMPERATURE OFFSET (°C)
L2774	-1	-
L2778	0	-1.074
L2976	-1	-0.015
L2977	-1	-0.010
L2784	0	-1.212
L2809	0	-0.187
L6811	-3	-0.003
L6814	-2	-0.010
L6812	-4	0.002
L6816	-3	0.015
L6817	-4	-0.001
L4653	-1	-0.016
L5705	8	-0.031
L5711	-2	0.002
L5710	-1	-0.034
L5701	4	-0.008
L5708	2	-0.023
L3810	-8	-0.108
L5704	0	-0.025
L6813	2	-0.007
L3578	-3	-0.127
L3806	0	-0.184
L3807	1	-0.162
L3804	-1	-0.175
L3805	-1	-0.160

L3809	0	-0.139

9.2. Median value of depth, temperature and salinity offset of the NKE sensors

Table 8. Median value of depth, temperature and salinity offset of the NKE sensors. The figures are rounded to the CTD accuracy.

SENSOR LABEL	DEPTH OFFSET (m)	TEMPERATURE OFFSET (°C)	SALINITY OFFSET (psu)
SP5149	-1	0.015	---
SP5269	0	-0.005	---
SP5150	0	0.010	---
SP5148	0	0.006	---
SP5151	0	0.030	---
SP5264	0	-0.013	---
SP5268	0	0.006	---
SP5270	0	0.005	---
SP5272	0	-0.006	---
STPS31003	0	0.002	-0.74
STPS31004	1	-0.007	0.12
STPS31005	-1	0.005	-0.22
STPS32001	0	-0.016	-0.14
STPS31006	-6	0.006	-0.18
STPS32002	0	-0.015	-0.02
STPS32003	0	-0.013	-0.26
STPS32005	0	-0.001	-0.04
STPS31002	-2	0.040	-0.22

9.3. Quality control algorithms for manual expert judgement– examples

9.3.1. Visual data editor with Matlab™ code from NOCS

Input:

File Names: jflag1.m, jflag2.m
Calls: jtest_flag10.m
Test data: jd10.mat, LAT10.mat, TEMP10.mat

Output:	**File description**
flag1_out.mat	generated by jflag1.m: holds latitude band information
susdat10.mat	generated by jflag1.m: stores the parameters' QC flags
suspcdatTEMP10_43_44.mat	generated by jflag2.m:stores each latitudes' QC flags
suspcdatTEMP10_50_51.mat	

Description:

This example shows a graphical method for determining outliers that relies on expert judgement. Data in the test data file are arranged as yearly vectors. These are plotted against time and latitude as in this case the route had a predominantly North – South orientation and had no duplicate latitudes within the same transect. It relies on the SOO occupying repeated transects to build up an annual distribution of values at each latitude.

Flags are produced for data that is visually determined to lie outside of an accepted range of values by graphical selection. Data are split into latitudinal bands of 1 degree and successively plotted to the screen with the option of editing.

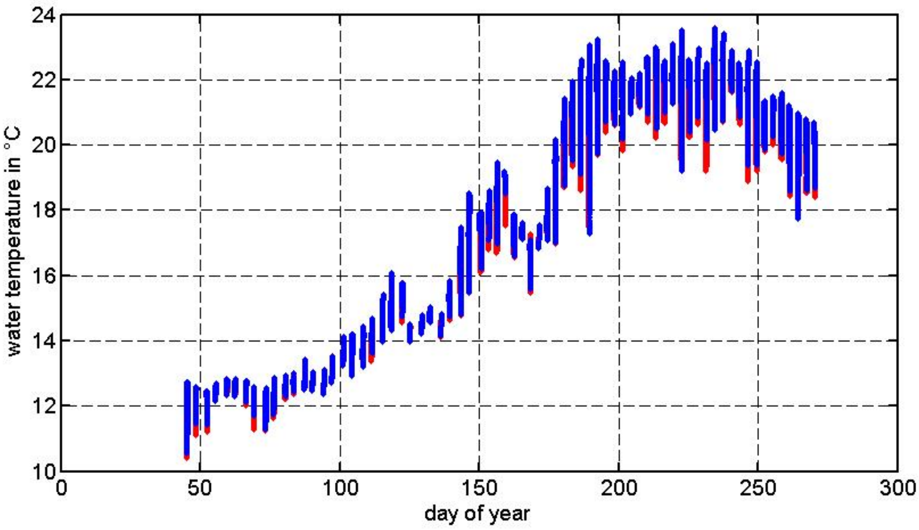

Figure 43 : Water temperatures from MS Pride of Bilbao (Bilbao-Portsmouth). Data are from route segment 43° to 44° N near the Bilbao harbour. Red filled circles are suspect data.

The data segment between 43° and 44° N is shown in Figure . Blue data points are good data, the red marked data are suspect and possibly bad data. The harbour of Bilbao is located at 43.335° N; thus, latitudes below that boundary are automatically flagged as suspect.

The next step in the algorithm is the choice of action by the user. When the results in the plot are satisfying, meaning that all data re probably good, the plot could be saved and printed; otherwise, the data and the plot could be edited.

```
Hit q to quit, e to edit, p to print, any other key to continue e
Editing
Choose from the following options:
k - horizontal zoom in with keyboard
m - horizontal zoom in with mouse
n - vertical zoom in with mouse
r - reset to view all data
s - select data to flag
q - save & quit
p - print current figure to file
e - exit without saving
v - view selected range (not finished yet)
b - break
l - continues with the next latitude band
Option: k
```

Figure 44 : Screenshot of Matlab™ algorithm for delayed data processing.

In this case, the plot can be zoomed before the selection of data that are to be flagged can be made. The action selection list in Matlab™ is shown in Figure . A selection of data that should be flagged is shown as an example in Figure . The frame can be placed manually in the plot. When the choice is declared satisfying in an interactive questionnaire in Matlab™'s command window, the data are flagged. This algorithm can be repeated as often as necessary.

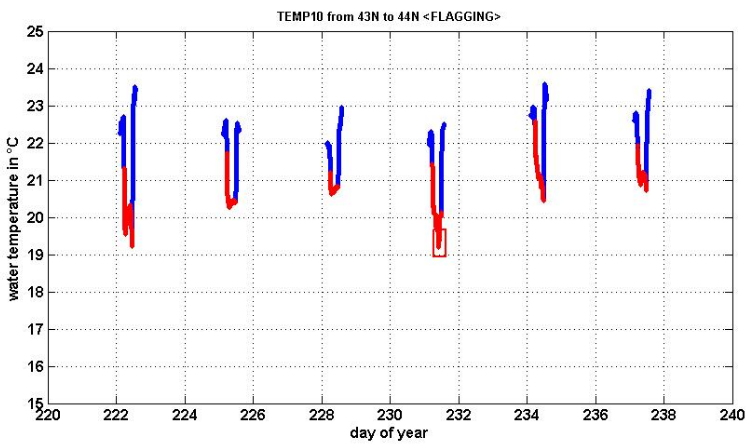

Figure 45 : Flagging of suspect water temperature data in Bilbao harbour.

9.3.2. *Visual data editor in HZG data base*

For the delayed data quality assessment an online tool for manual data flagging is available. So, for additional flagging after the initial real-time quality control process this proves to be a powerful quality control instrument.

Starting from the HZG data base web tool, the data assessment centre gives several possibilities for quality control.

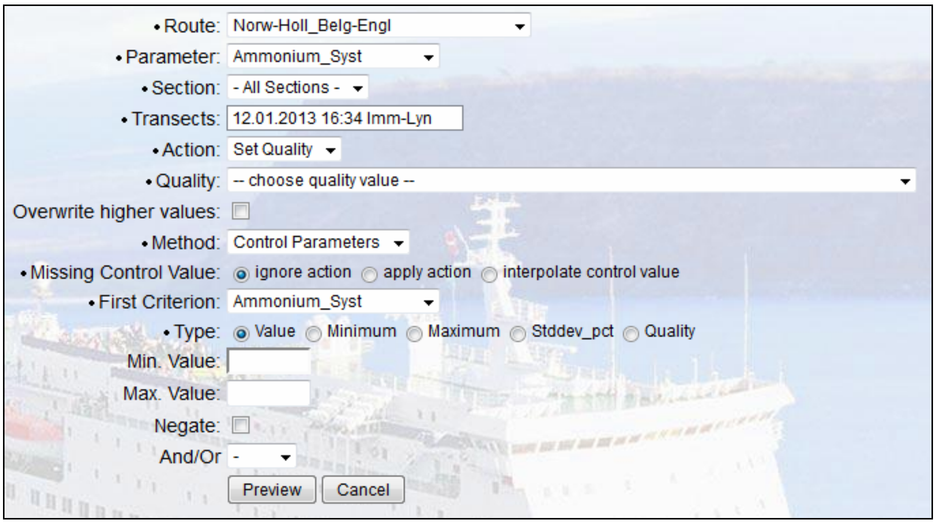

Figure 46 : Selection window of the data assessment at HZG online data base. In this case, the method Control Parameters is selected. For other methods, also some other options are present.

Besides the choice of the FerryBox route and individual transects, the action of assessment can be selected: either the data are flagged or they are deleted from the data base.

The flagging is made according to the FerryBox data flags standard, shown in Table. The selection can be made at “quality – choose quality value” in Figure .

There are four possible Methods available:

- Control parameters
- After departure
- Frozen Values
- After Restart

- Range

In case of the Control parameters option, the parameter criterion can be selected among the measured FerryBox parameters, the type of value (i.e. value or stddev etc.) and the allowed value range of the parameter criterion. A useful criterion is e.g. the flow rate.

For the After departure and the Frozen value options, the duration of the flagging period can be selected.

For the After Restart option, a control parameter (e.g. the flow rate), the duration in minutes of the gap period and of the after gap period can be chosen.

For the Range option, the distance in kilometres can be selected.

In the following, examples of data flagging are shown.

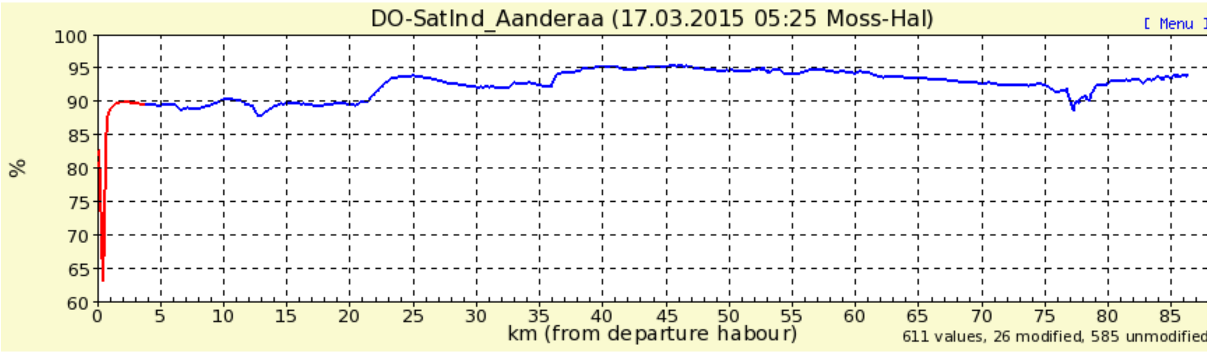

Figure 47 : Flagging of dissolved oxygen data after departure from harbour Moss/Norway. Red line indicates the flagging to value -1 (bad data).

Figure 47 depicts the dissolved oxygen FerryBox data between route Moss-Halden, scaled by the distance from on harbour to the next. The after departure time period has been selected to be 10 minutes. Data that are in this period are flagged and shown in Figure as red line.

The flagging of frozen values are shown in figure 48 for pH data taken on the ferry route from Büsum to Helgoland in the German bight. The time period of frozen status was selected to be at least 10 minutes. In this figure, the frozen status lasts longer, so the first 48 km of the transect have been flagged, shown as a red line.

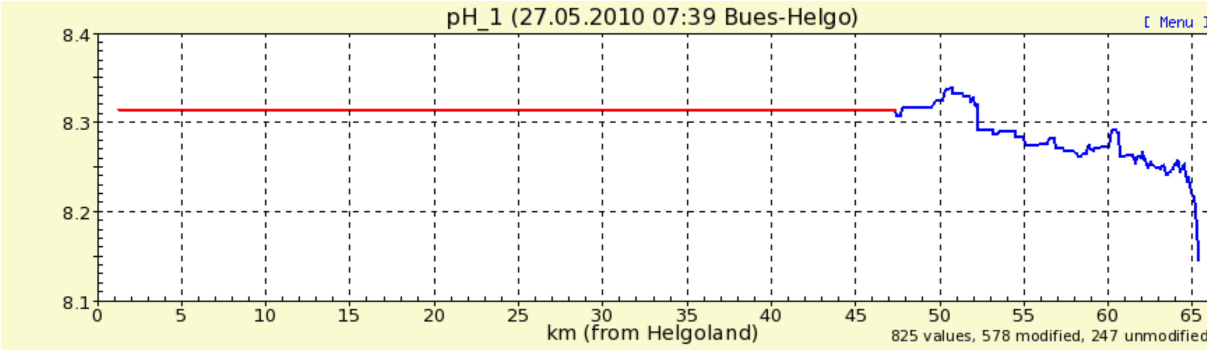

Figure 48 : Flagging of pH data due to frozen values at FerryBox route Büsum-Helgoland (Germany). Red line indicates the flagging to value -1 (bad data).

For the flagging of after restart cases, a control parameter is needed. In this case, the flow rate in the pumping system is used, as this a common method. Figure 49 shows the transect data of the flow rate in the FerryBox of the route between Halden(NO) to Zeebruegge(BE). There is clearly seen a gap ranging to nearly 20 km of no data. At km 50, the FerryBox was restarted. In Figure, corresponding xCO_2 data are depicted. They have been flagged due to the FerryBox restarting, notified by the flow rate. In the main window selection the gap had to be at least 30 minutes and the duration after the gap should be 15 minutes. In this time period, xCO_2 data are treated as bad data (value=-1), after that, they were flagged as good data (value=8).

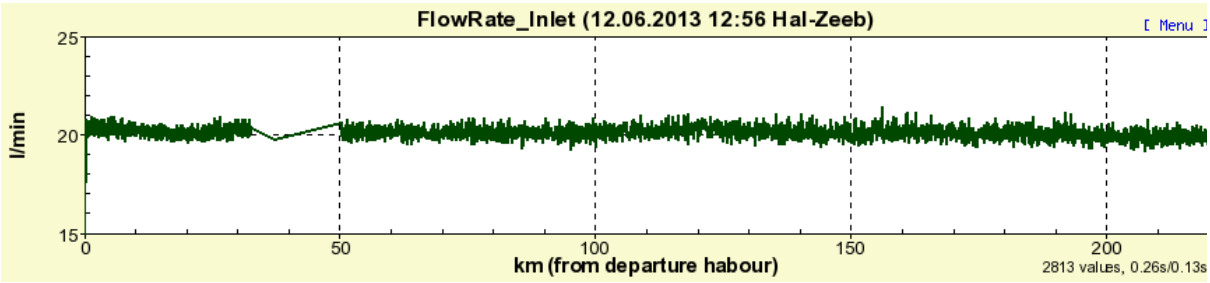

Figure 49 : Control parameter flow rate for After Restart data flagging.

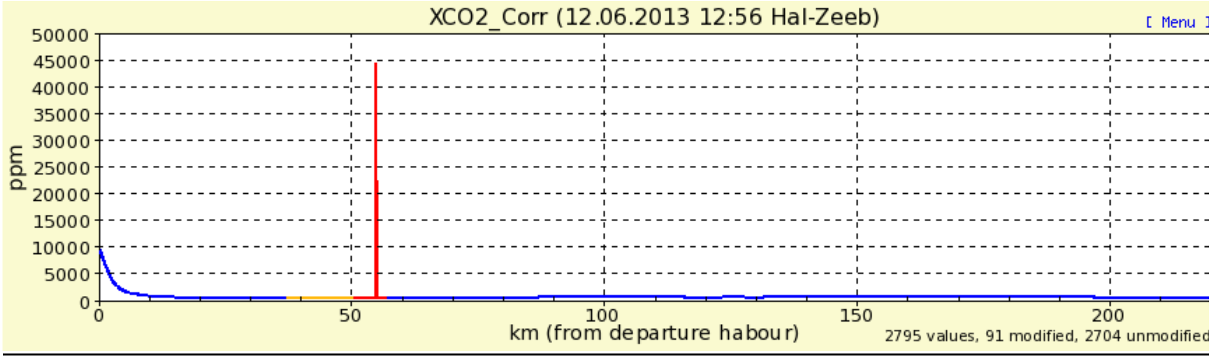

Figure 50 : Flagging of xCO_2 data due to after restart period (shown in yellow). Flagged data for FerryBox route Halden(NO)-Zeebruegge(BE) are shown in red.

For the control parameter flagging, an example is shown of the FerryBox route Cuxhaven(GER)-Immingham(UK) for the year 2012. In Figure 51, the flow rate is depicted for the transect with bad data showing at the beginning of the transect. While the flow rate is stable around 18 l/min for the main parts of the transect, it varies strongly at the transect start. Thus, the corresponding turbidity data in Figure 52 were flagged. In the main selection window, only flow rates between 10 and 30 l/min are allowed to be flagged as good data (value=8), outside of this range, turbidity data are flagged as bad data (value=-1). Thus the spiked data in Figure 52 have been flagged according to the flow rate parameter.

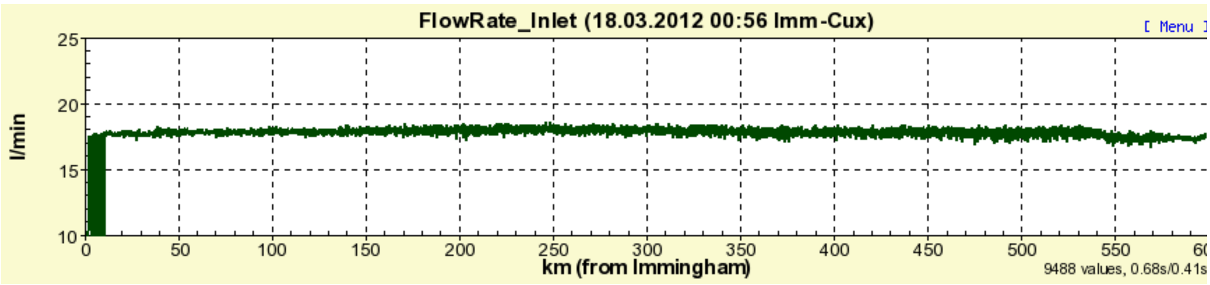

Figure 51 : Control parameter flow rate for data flagging.

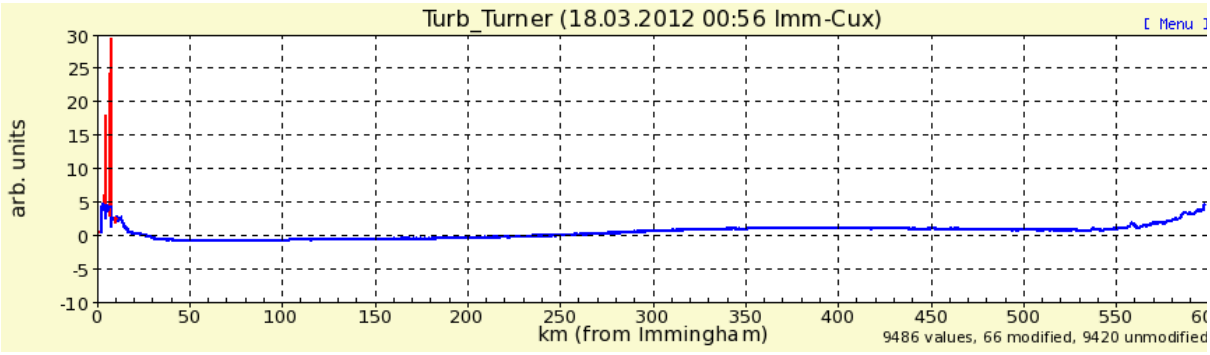

Figure 52 : Flagging of turbidity data due to control parameter flow rate for FerryBox route Cuxhaven(GER)-Immingham(UK). Red line indicates bad data.